Development 140, 2619-2631 (2013) doi:10.1242/dev.091355

ASCL1 reprograms mouse Müller glia into neurogenic retinal progenitors

Julia Pollak[1,2], Matthew S. Wilken[1,3], Yumi Ueki[1], Kristen E. Cox[1], Jane M. Sullivan[2,4], Russell J. Taylor[1], Edward M. Levine[5] and Thomas A. Reh[1,2,3,*]

SUMMARY

Non-mammalian vertebrates have a robust ability to regenerate injured retinal neurons from Müller glia (MG) that activate the gene encoding the proneural factor Achaete-scute homolog 1 (*Ascl1*; also known as *Mash1* in mammals) and de-differentiate into progenitor cells. By contrast, mammalian MG have a limited regenerative response and fail to upregulate *Ascl1* after injury. To test whether ASCL1 could restore neurogenic potential to mammalian MG, we overexpressed ASCL1 in dissociated mouse MG cultures and intact retinal explants. ASCL1-infected MG upregulated retinal progenitor-specific genes and downregulated glial genes. Furthermore, ASCL1 remodeled the chromatin at its targets from a repressive to an active configuration. MG-derived progenitors differentiated into cells that exhibited neuronal morphologies, expressed retinal subtype-specific neuronal markers and displayed neuron-like physiological responses. These results indicate that a single transcription factor, ASCL1, can induce a neurogenic state in mature MG.

KEY WORDS: Müller, Glia, Neurogenesis, Regeneration, Reprogramming, Retina

INTRODUCTION

Many non-mammalian vertebrates have the ability to regenerate new neurons after retinal injury. In fish, initially quiescent MG respond to chemical- or light-induced damage by re-entering the cell cycle and de-differentiating to form multipotent progenitors; these progenitors give rise to all retinal neuron subtypes and repair the lost neurons (Raymond et al., 2006; Bernardos et al., 2007; Fausett et al., 2008; Thummel et al., 2008; Ramachandran et al., 2010). However, mammals have a restricted ability to regenerate the retina. In rodents, MG can form new neurons in response to damage and growth factor stimulation, but only in very limited numbers (Ooto et al., 2004; Close et al., 2006; Osakada et al., 2007; Wan et al., 2008; Takeda et al., 2008; Karl et al., 2008; Del Debbio et al., 2010). Instead, mammalian MG normally respond to damage by becoming reactive and undergoing gliosis (Bringmann et al., 2009; Dyer and Cepko, 2000). We are interested in finding mechanisms to enhance the regenerative response of mammals, and recent advances in somatic cell reprogramming towards neural fates have potential application in the mammalian retina.

Recent reports have demonstrated highly efficient conversion between distant cell lineages using a minimal number of transcription factors (Vierbuchen and Wernig, 2011). Glial cells are ideal candidates for reprogramming, as they share many properties with progenitor cells (Berninger, 2010; Nelson et al., 2011). In astrocytes, forced expression of a number of transcription factors promotes neuronal conversion (Heins et al., 2002; Berninger et al., 2007; Blum et al., 2011; Heinrich et al., 2010; Addis et al., 2011; Corti et al., 2012). Moreover, Ascl1 is emerging as a key factor involved in neuronal fate conversion. Vierbuchen et al. (Vierbuchen et al., 2010) demonstrated that viral expression of *Ascl1* along with two other transcription factors, *Brn2* (*Pou3f2* – Mouse Genome Informatics) and *Myt1l*, could directly convert fibroblasts into neurons, although *Ascl1* alone was sufficient to induce significant conversion.

Recently, Ascl1a was shown to be required for retinal regeneration in the fish. *ascl1a* is upregulated in proliferating MG within six hours of injury, and Ascl1a knockdown blocks MG proliferation and de-differentiation into progenitors (Fausett et al., 2008; Ramachandran et al., 2010; Ramachandran et al., 2012; Wan et al., 2012). Because *Ascl1* is not upregulated in the mouse retina after N-methyl-D-aspartate (NMDA)-induced damage (Karl et al., 2008), we hypothesized that the limited regenerative capacity of mammalian MG might be due, in part, to their failure to activate Ascl1 after damage. Further support for this hypothesis is demonstrated by the neurogenic role of Ascl1 during normal retinal development. In the developing mouse retina, Ascl1 maintains progenitors by driving expression of components of the Notch pathway (Nelson et al., 2009; Jasoni and Reh, 1996). Knockout of *Ascl1* increases the number of MG relative to other cell types (Tomita et al., 2000; Akagi et al., 2004), whereas Ascl1 overexpression in progenitors biases cell production towards photoreceptor, and possibly bipolar, cells in mice (Hatakeyama et al., 2001), amacrine cells in the chick (Mao et al., 2008), and bipolar and amacrine cells in human cells (Gamm et al., 2008).

In the present study, we demonstrate that viral expression of ASCL1 is sufficient to activate a neurogenic program in mammalian MG, both in dissociated cultures and in the intact retina. ASCL1 remodels the chromatin at retinal progenitor genes, activates their expression and downregulates glial genes. The reprogrammed MG differentiate into cells that resemble neurons in morphology, gene expression and their responses to neurotransmitters. Our results suggest that stimulating neurogenesis in MG with ASCL1 could provide an alternative strategy for repair of the retina after disease or injury.

[1]Department of Biological Structure, University of Washington, Seattle, WA 98195, USA. [2]Neurobiology and Behavior Program, University of Washington, Seattle, WA 98195, USA. [3]Molecular and Cellular Biology Program, University of Washington, Seattle, WA 98195, USA. [4]Department of Physiology and Biophysics, University of Washington, Seattle, WA 98195, USA. [5]Department of Ophthalmology and Visual Sciences, John A. Moran Eye Center, University of Utah, Salt Lake City, UT 84132, USA.

*Author for correspondence (tomreh@u.washington.edu)

Accepted 3 April 2013

MATERIALS AND METHODS

Animals

Mice were housed at the University of Washington; protocols were approved by the University of Washington Institutional Animal Care and Use Committee. C57BL/6J mice (Jackson) were used except where indicated. *Hes5-GFP* mice (Basak and Taylor, 2007) have been previously characterized as an MG reporter line *in vivo* and for fluorescence-activated cell (FAC)-sorting (Nelson et al., 2011). *Rlbp1-cre*^{ERT2} mice were derived from plasmid described by Vázquez-Chona et al. (Vázquez-Chona et al., 2009) and were crossed to *R26-stop-flox-CAG-tdTomato* mice (Jackson). α*Pax6-cre* mice (R. Ashery-Padan, Tel-Aviv University, Tel-Aviv, Israel) (Marquardt et al., 2001) were crossed to *R26-stop-flox-rtTA* mice (Jackson) (Belteki et al., 2005). NMDA damage was performed as previously described (Ueki et al., 2012). Tamoxifen (Sigma) was administered intraperitoneally at 100 mg/kg in corn oil.

Plasmids and viral production

PLOC-hASCL1-IRES-turboGFP(nuc) (Open Biosystems) was used to generate *PLOC-IRES-turboGFP*(nuc). *hASCL1-IRES* sequence was inserted into the *pTRE3G-mCherryn* vector (Tet-On 3G, Clontech), and inserted into the *pLVX-Tight-Puro* vector (Clontech) using In-Fusion Cloning (Clontech). *pLVX-Tet-On Advanced* (Clontech) was used to express rtTA protein *in vitro*.

Dissociated MG culture

MG from postnatal day (P)12 mice were cultured [Neurobasal + N2, epidermal growth factor (EGF), 10% fetal bovine serum (FBS)] as previously described (Ueki et al., 2012) with 1 μM 5-ethynyl-2′-deoxyuridine (EdU). Lentiviral particles were added in Optimem (Gibco) or neural medium (Neurobasal + N2, B27, 1% tetracycline (tet)-free FBS), and 3-6 hours later medium was replaced. hBDNF (R&D Systems, 10 ng/ml), bFGF (R&D Systems, 100 ng/ml) and rGDNF (R&D Systems, 10 ng/ml) were added for longer cultures. 4-Hydroxytamoxifen (4-OHT; Sigma) was included where indicated at 10 μM.

Retinal explants

Retinas of α*Pax6-cre;R26-stop-flox-rtTA* mice were explanted at P12 as previously described (Ueki et al., 2012). Explants were infected with *pLVX-tetO-hASCL1-IRES-mCherryn*, and 3 μg/ml doxycycline was added at 2 days *in vitro* (div).

Reverse transcriptase quantitative PCR (qPCR) and microarray analysis

Cells were lysed in Trizol (Invitrogen), and RNA was extracted, followed by DNase-1 (Qiagen) digestion and RNA cleanup (Qiagen). Microarray data were generated using GeneChip Mouse Gene 1.0 ST Array (Affymetrix) at the Institute for Systems Biology (Seattle, WA, USA) (see Nelson et al., 2011). Microarray data were deposited in Gene Expression Omnibus under accession number GSE45835. cDNA was synthesized (iScript cDNA Synthesis Kit, Bio-Rad), and qPCR was performed (SsoFast EvaGreen Supermix, Bio-Rad) on a Bio-Rad thermocycler. Reactions were performed in triplicate and values normalized to *Actb*. ΔΔCt between ASCL1-infected and uninfected or GFP-infected MG was expressed as fold change ($2^{\Delta\Delta Ct}$). Standard error of the mean (s.e.m.) was determined from ΔΔCt values and log transformed. One-way Student's *t*-test was performed on ΔΔCt values compared with 0 (Yuan et al., 2006). qPCR primers are listed in supplementary material Table S1.

Chromatin immunoprecipitation (ChIP)

For Ascl1 ChIP, P0 retinas or cultured P12 MG were digested with papain into a single cell suspension and fixed with 1% formaldehyde for 10 minutes at room temperature (RT). Cells were sonicated at 4°C. Ascl1 IP was performed with 40 μl anti-mouse IgG magnetic beads (Invitrogen) and 4 μg mouse anti-Mash1 antibody (BD Pharmingen) or 4 μg mouse IgG (Millipore) against chromatin from 1×10^6 (P0 retinas) or 2.5×10^5 (cultured MG) cells per IP according to LowCell # ChIP Kit (Diagenode). IP and wash buffers were as described by Castro et al. (Castro et al., 2006). DNA sequences were quantified by qPCR and averaged from three to six independent experiments. For histone ChIP, cell suspensions were fixed with 0.5% formaldehyde (10 minutes at RT) and sonicated. IP was performed with 20 μl anti-rabbit IgG magnetic beads (Invitrogen) and 2 μg rabbit anti-H3K27me3 (Active Motif), rabbit anti-H3K27Ac (Abcam) or rabbit IgG (R&D Systems). Values were averaged from three to five independent experiments. See supplementary material Table S1 for ChIP primers.

Western blot

Cells were collected in lysis buffer and processed as described by Ueki et al. (Ueki et al., 2012). Antibodies used were: anti-Cralbp (1:5000; Abcam), anti-glutamine synthetase (1:10,000; Millipore), anti-β-actin (1:10,000; Abcam) and horseradish peroxidase-conjugated goat anti-mouse (1:10,000; Bio-Rad).

Immunofluorescence

Coverslips were fixed in 2% paraformaldehyde (PFA) and standard protocols were used (Ueki et al., 2012). EdU staining was carried out using the Click-iT EdU Kit (Invitrogen). Explants were fixed in 2% PFA and immunolabeled as whole mounts. For cryosections, retinas were fixed in 2% PFA and sectioned at a thickness of 12 μm. Primary antibodies used were: anti-Insm1 (1:100; Genway), anti-Mash1 (1:100; BD Biosciences), anti-Ascl1 (1:250; Gift of J. Johnson, UT Southwestern, TX, USA), anti-GsiB4 Lectin (1:500; Vector Laboratories), anti-calretinin (1:1000; Swant), anti-Cralbp (1:1000; Gift of J. Saari, University of Washington, WA, USA), anti-RFP (1:500; Clontech), anti-RFP (1:500; Abcam), anti-Tuj1 (1:500; Covance), anti-Map2 (1:200; Sigma M9942), anti-S100β (1:1000; Sigma), anti-GFP (1:500; Abcam), biotinylated anti-Otx2 (1:100; R&D Systems), anti-Islet1 (1:50; Developmental Studies Hybridoma Bank), anti-Sox2 (1:250; Abcam), anti-Sox2 (1:250; Santa Cruz), anti-Id1 (1:200; BioCheck), anti-Pax6 (1:600; Covance), anti-Hes5 (1:100; Santa Cruz), anti-Sox9 (1:500; Millipore), anti-phospho-histone H3 (PH3) (1:500; Millipore), anti-NG2 (1:100; Chemicon). Secondary antibodies from Invitrogen, Molecular Probes and Jackson ImmunoResearch were used at 1:400 or 1:500.

Microscopy and cell counting

Imaging was performed using an Olympus Fluoview confocal microscope or Zeiss Observer D1 with AxioCam. Three to six random fields per coverslip (20×) were counted. Single slice images (1 μm thick) were counted from four to eight random fields per explant. Seven explants were analyzed for each neuronal marker. *z*-stacks (0.5 μm thick per slice) were also captured to analyze colocalization of signals in three dimensions. Time-lapse imaging was performed on an Axio Observer Z1 (Zeiss) using Axiovision 4.7 software (Zeiss); CO_2, O_2 and temperature were kept at standard cell culture conditions.

Ratiometric Ca^{2+} imaging

Dissociated cells on coverslips were incubated in a solution of Fura-2 (Invitrogen) and Pluronic F-127 (Invitrogen) in Hank's balanced salt solution (HBSS+) (Gibco) for 30 minutes at 30°C, then washed in HBSS+ for 30 minutes. Chemicals (NMDA, 100 μM; glycine, 10 μM; kainate, 10 μM; ATP, 100 μM; KCl, 50 mM; all obtained from Sigma) were diluted in HBSS and applied by bath perfusion at constant flow rate for 60 seconds at 30°C before a 60-second washout with HBSS. Images were taken every 4 or 6 seconds at 340 and 380 nm alternating excitation, and ratios of fluorescence intensity signals (F340/380) were determined (Metafluor; Molecular Devices). F340/380 values were normalized to baseline activity. Each experiment was conducted on multiple coverslips over multiple days, and at least three experiments were conducted for each agonist.

Electrophysiology

Whole-cell voltage clamp and current clamp recordings were made from ASCL1-GFP-expressing cells using an Axopatch 200B amplifier (Molecular Devices). Electrodes (2-4 MΩ) were filled with 148.5 mM potassium gluconate, 9 mM NaCl, 1 mM $MgCl_2$, 10 mM HEPES and 0.2 mM EGTA (330 mOsm, pH 7.2). The extracellular solution contained 119 mM NaCl, 5 mM KCl, 2.5 mM $CaCl_2$, 30 mM glucose, 20 mM HEPES and 1 μM glycine. Action potentials were elicited by injecting current into cells in whole-cell current clamp mode. Responses to 50 μM kainate (in extracellular solution) were recorded in response to 3-8 seconds of drug

application, delivered with a local puffer pipette controlled by a Picospritzer (Parker Hannifin) while holding the membrane at –60 mV under voltage clamp. Spontaneous miniature postsynaptic currents were recorded during continuous 10-second sweeps while holding the membrane at –60 mV under voltage clamp.

RESULTS

Viral-mediated overexpression of ASCL1 in MG cultures

To study efficient transcription factor-mediated conversion, we needed a reliable and well-characterized cell culture model of mouse MG. We recently demonstrated that MG from postnatal day 11-12 (hereafter referred to as P12) mouse retina have mature glial properties and can expand as dissociated cultures (Ueki et al., 2012). By this age, all of the progenitors have completed their final mitotic cell divisions and differentiated as retinal neurons or MG. Upon retinal dissociation, most neurons die within one day, and only a small number survive after initial passage. MG proliferate over the next week, and >95% of cells express common MG markers after 4-5 days *in vitro* (div). Other cell types were not found to be a major source of contamination by immunolabeling and microarray analysis for astrocyte-, neuron- and endothelial-specific markers (Ueki et al., 2012), as well as by immunolabeling for the pericyte marker NG2 (Cspg4 – Mouse Genome Informatics) (supplementary material Fig. S1A).

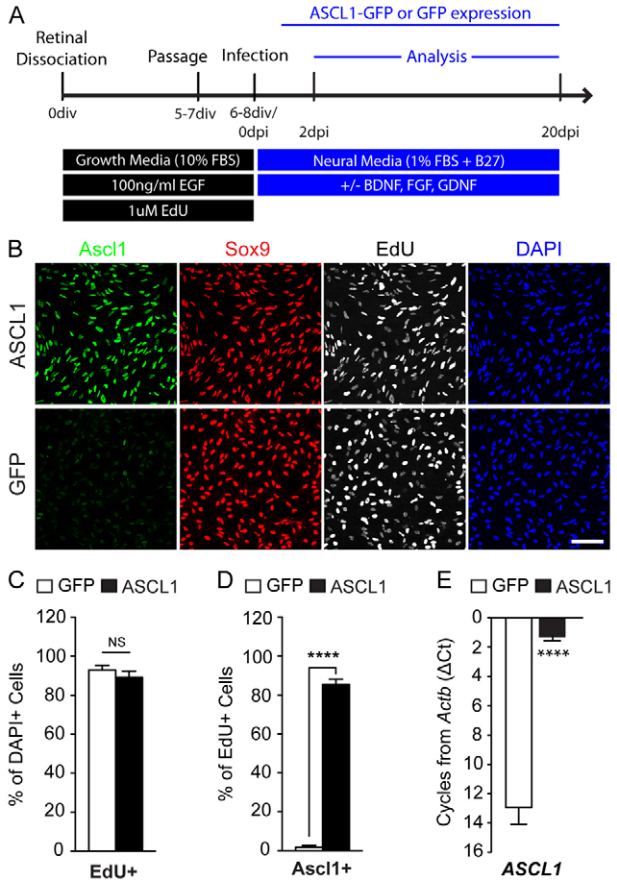

Fig. 1. Viral-mediated ASCL1 expression in dissociated MG cultures. (**A**) Experimental design. (**B**) ASCL1-infected P12 MG express Sox9 (red), incorporate EdU (white) and express Ascl1 protein (green) (4 dpi). GFP-infected MG do not express Ascl1. Scale bar: 100 µm. (**C**) ASCL1- and GFP-infected MG incorporate EdU (4-5 div). (**D**) ASCL1-infected EdU+ MG express Ascl1 (4-5 dpi). (**E**) Human *ASCL1* mRNA in ASCL1-infected P12 MG at 4 dpi by qPCR. Data are mean±s.e.m. NS, not significant, ****P<0.0001; Student's t-test.

To test whether ASCL1 was sufficient to reprogram MG into neurogenic progenitors, we carried out the experimental design detailed in Fig. 1A. P12 MG were cultured for one week, and EdU was added throughout this period to distinguish MG and their progeny from surviving post-mitotic neurons. Cells were passaged to remove surviving neurons and then infected with lentiviral particles expressing GFP or ASCL1-GFP in neural medium (1% FBS + B27). More than 85% of P12 MG had incorporated EdU by 4 days post-infection (dpi) (~10 div), in both GFP and ASCL1-infected cultures (Fig. 1B,C). Ascl1 expression was robust at 4 dpi; 85.4±2.7% of EdU+ ASCL1-infected P12 MG expressed Ascl1 protein compared with 1.8±0.9% of GFP-infected MG (Fig. 1B,D). At 4 dpi, *ASCL1* mRNA was highly expressed; Fig. 1E shows the qPCR for human *ASCL1* in ASCL1-infected cultures compared with paired GFP-infected cultures. ASCL1-infected MG had >2^{11} times (2000-fold) more *ASCL1* than the GFP-infected MG.

ASCL1-infected MG express retinal progenitor-specific genes

Because P12 MG do not normally express Ascl1, we initially assessed whether ASCL1 would bind to its predicted targets (Nelson et al., 2009; Castro et al., 2011) in these cells after overexpression. Chromatin immunoprecipitation (ChIP) with an Ascl1 antibody was performed in newborn mouse retina, when endogenous *Ascl1* and its predicted targets are highly expressed (Fig. 2A, gray bars). There was significant pull-down of Ascl1 at the promoters of *Dll3*, *Hes6*, *Mfng*, *Hes5* and *Dll1* in P0 retina. Predictably, these targets were not enriched for Ascl1 in GFP-infected P12 MG (supplementary material Fig. S2). However, 4 days after ASCL1 infection, Ascl1 was significantly enriched at these promoters (Fig. 2A; supplementary material Fig. S2, blue bars), indicating that ASCL1 can bind its developmental targets in P12 MG.

Next, microarray analysis was used to understand the extent to which ASCL1 may activate developmental expression patterns in the infected MG. Although many progenitor genes are normally expressed in MG, we recently characterized a subset of genes, primarily proneural factors and Notch pathway components, that are highly expressed in Hes5– GFP+ FAC-sorted progenitors, but not in MG (Nelson et al., 2011). In Fig. 2B, we compared the expression levels of these genes in Hes5– GFP+ retinal progenitors (P0 RPCs) with those in dissociated P12 MG cultures infected with GFP or ASCL1 at 4 dpi. ASCL1 induced the expression of many of these progenitor-specific genes in P12 MG. Many of the genes that are highly upregulated in ASCL1-infected glia are known targets of Ascl1, such as *Dll1*, *Dll3*, *Hes5*, *Hes6*, *Gadd45g*, *Fabp7*, *Id1*, *Id3* and *Mfng*, whereas others are not known Ascl1 targets, e.g. *Neurog2*, *Mycn*, *Olig2* and *Fgf15*. The Notch pathway genes *Heyl*, *Hey1*, *Hes1* and *Dner* were also increased. A gene ontology (GO) analysis of the genes that were upregulated in MG after ASCL1 infection (Eden et al., 2007; Eden et al., 2009) revealed that the biological function terms with the highest P-values were those associated with 'nervous system development' and 'regulation of neurogenesis'; terms related to synaptic transmission, conduction of nerve impulses and cell cycle/DNA replication were also enriched in the genes upregulated in ASCL1-infected MG cells (supplementary material Table S2). Although these changes are consistent with ASCL1 reprogramming MG to the retinal progenitor state, not all progenitor-specific genes were upregulated by ASCL1 infection (supplementary material Fig. S3). Genes expressed

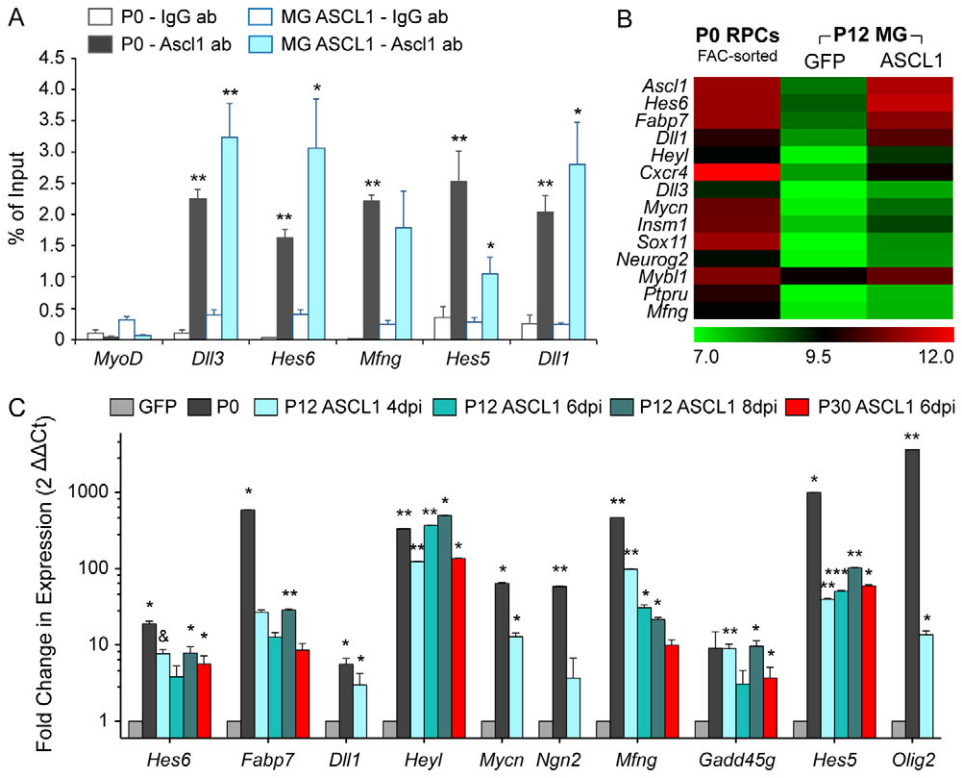

Fig. 2. ASCL1 induces progenitor gene expression in MG. (**A**) ChIP, shown as percentage of input DNA, for Ascl1 or IgG antibodies at the 5′ promoter of the genes indicated. Significance was tested against values at the *MyoD* promoter, the negative control. (**B**) Microarray analysis comparing *Hes5-GFP* FAC-sorted P0 retinal progenitor cells (RPCs) to ASCL1- or GFP-infected P12 MG (4 dpi). The expression levels are log transformed and normalized. (**C**) qPCR of progenitor genes upregulated on the microarray. ASCL1- and GFP-infected MG from P12 mice at 4, 6 or 8 dpi or NMDA-damaged P30 mice at 6 dpi. Data are mean±s.e.m. **P*<0.05, ***P*<0.01, ****P*<0.001, &*P*<0.0001; Student's *t*-test.

specifically in early embryonic retinal progenitors, such as *Hmgb3* and *Sfrp2*, are examples of genes that were not increased.

These changes in gene expression were then validated by qPCR by comparing expression levels of progenitor genes in infected MG relative to those present during development. Figure 2C shows levels of expression in newborn (P0-P1) mouse retina or ASCL1-infected P12 MG relative to GFP-infected P12 MG. At 4 dpi, there was very good correspondence between increases in gene expression observed in the microarray data and the qPCR experiments. Almost all genes were significantly increased in ASCL1-infected P12 glia at 4 dpi, though in most cases the level of expression did not reach that observed in the P0 progenitors. At 6 and 8 dpi, progenitor genes were still expressed in ASCL1-infected glia; however, by 13 dpi, the level of the most highly upregulated genes, *Hes5*, *Mfng* and *Heyl*, were decreased (supplementary material Fig. S4). These data suggest that the induction of progenitor genes in MG by ASCL1 infection is, in part, transient.

To test whether similar changes could be induced in MG from adult retinas, we used a recently developed protocol to isolate MG from adult (P30) mouse retina after NMDA-induced neurotoxic damage to the neurons. Adult glia from NMDA-damaged retinas proliferated *in vitro*, and the majority of cells were labeled with EdU and the glial marker S100β (supplementary material Fig. S1B). Typically <1% of the cells in the cultures were isolectin B4+ endothelial cells (supplementary material Fig. S1B). When adult MG were infected with ASCL1, we found similar levels of activation of progenitor genes as in P12 MG (Fig. 2C, red bars).

Microarray and qPCR results were further validated using immunofluorescence. *Hes5*, *Insm1* and *Dll1* are highly expressed in developing retinal progenitors (Nelson et al., 2007; Nelson et al., 2009) and are not highly expressed in MG *in vivo* or *in vitro* on our microarray analysis. By contrast, after 4 days of ASCL1 overexpression ~15% of EdU+ P12 MG were immunoreactive for Hes5 (Fig. 3A,B) or Insm1 (Fig. 3C,D) with a smaller percentage (~10%) immunoreactive for Dll1 (not shown). The percentage of Hes5+ cells remained relatively constant from 3 to 7 dpi, consistent with the qPCR time course data.

The GO analysis of the microarray data further suggested that ASCL1-infected MG have a higher level of some cell cycle genes. Time-lapse recordings of the MG after ASCL1 infection showed that the infected cells continued to undergo mitotic divisions (Fig. 4A), and ASCL1-infected MG had a greater number of cells expressing the mitotic marker PH3 (Fig. 4B,C). Approximately 50% of these PH3+ cells also expressed the progenitor marker Hes5 (Fig. 4D).

ASCL1 remodels target gene chromatin in P12 MG

The fact that ASCL1 is able to directly bind the promoters and/or proximal enhancers of progenitor genes *Hes5*, *Dll1*, *Hes6* and *Dll3* and activate their expression suggests that chromatin at these sites can be reprogrammed to an active state by ASCL1. To determine directly the chromatin status at progenitor genes, we probed the 5′ proximal regions of these genes for active and repressive histone modifications in both P0 retinal progenitors and P12 MG. Histone 3 lysine 27 tri-methylation (H3K27me3) represses expression of genes with this histone modification (Cao et al., 2002; Boyer et al., 2006), whereas H3K27 acetylation (H3K27Ac) is correlated with the promoters and enhancers of actively expressed genes (Karlić et al., 2010). ChIP-qPCR was performed for both modifications at the 5′ proximal promoters (or 5′ enhancer for *Dll1*). We observed a significant increase in the repressive H3K27me3 modification (Fig. 5A) and a significant decrease in the active H3K27Ac modification (Fig. 5B) between progenitors and MG at all four gene loci.

Because repressive chromatin modifications are established at genes that can be subsequently activated by ASCL1, we reasoned that ASCL1 might reprogram the chromatin at these gene loci from a state of repression to activation. We therefore performed ChIP for

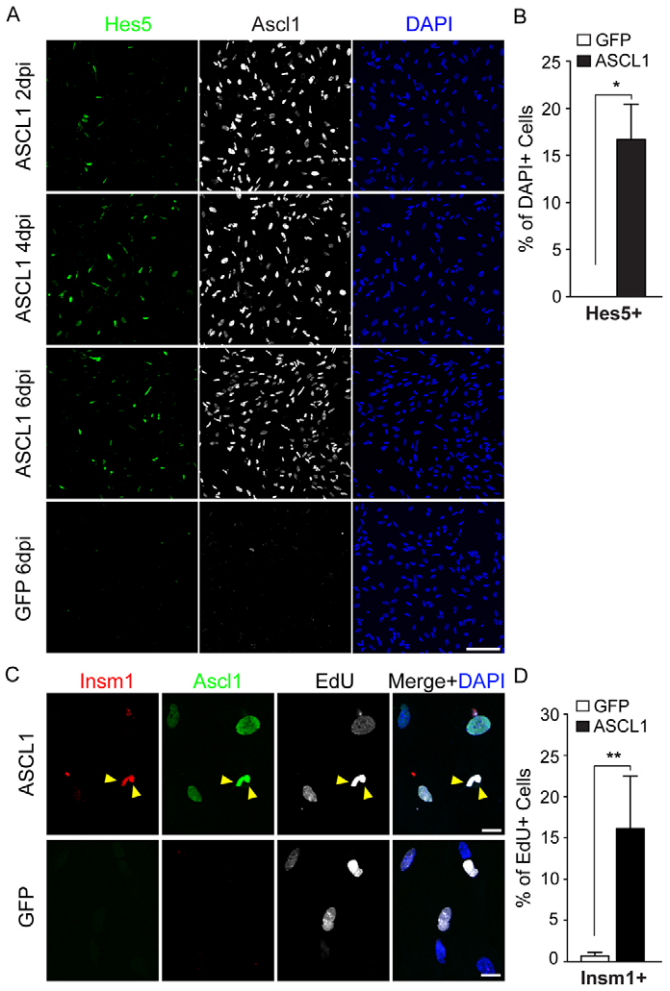

Fig. 3. ASCL1-infected MG express markers of retinal progenitors. (**A**) ASCL1+ cells express Hes5 from 2 to 6 dpi. Hes5+ cells are absent from GFP-infected MG. (**B**) Graph of Hes5+ cells in ASCL1- and GFP-infected MG (4 dpi). (**C**) ASCL1-infected ASCL1+EdU+ MG express the progenitor marker Insm1 (4 dpi) (arrowheads indicate triple-labeled cells). (**D**) Insm1+EdU+ cells are increased in ASCL1-infected MG (4-5 dpi). Data are mean±s.e.m. **P*<0.05, ***P*<0.01; Student's *t*-test. Scale bars: in A, 100 μm; in C, 20 μm.

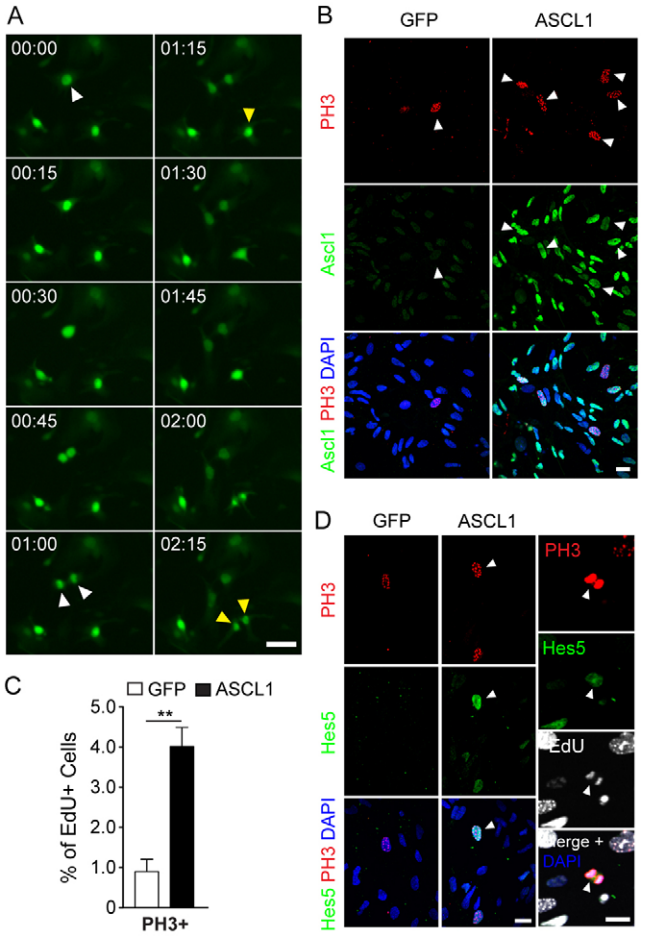

Fig. 4. ASCL1+ MG-derived cells proliferate. (**A**) Time-lapse imaging of ASCL1-infected MG starting at 7 dpi. Two examples of ASCL1– GFP+ cells dividing are indicated with arrowheads. (**B**) ASCL1+ MG express PH3 (red) at 4 dpi. PH3+ cells in GFP-infected MG are ASCL1–. Arrowheads indicate double-labeled cells. (**C**) PH3+EdU+ cells are increased in ASCL1-infected MG compared with GFP-infected MG at 4 dpi. (**D**) Hes5+ progenitors express PH3 and divide (right panel) in ASCL1-infected cells at 4 dpi. Data are mean±s.e.m. ***P*<0.01; Student's *t*-test. Scale bars: 20 μm.

H3K27me3 and H3K27Ac on dissociated P12 MG infected with ASCL1 or GFP at 4 dpi. We observed a significant decrease in H3K27me3, except at *Hes6* (Fig. 5C), and an increase in H3K27Ac (Fig. 5D) at progenitor gene loci in ASCL1-infected MG. These data demonstrate that ASCL1 has the ability to bind genes with repressed chromatin and reprogram the chromatin to an active state.

We also assessed the chromatin state of the Ascl1 promoter in MG. We found that, like its targets, the promoter of Ascl1 acquires the H3K27me3 repressive histone modification in MG, unlike in P0 retinal progenitors (supplementary material Fig. S5A), while at the same time losing the H3K27Ac active modification (supplementary material Fig. S5B). Overexpression of ASCL1 in MG was able to partly remodel the Ascl1 promoter, causing an increase in the H3K27Ac modification (supplementary material Fig. S5D); however, there was a persistence of the repressive modification H3K27me3 at these loci (supplementary material Fig. S5C), which might prevent significant expression of endogenous Ascl1 in the reprogrammed MG.

ASCL1-infected MG lose glial properties

Because ASCL1-infected MG robustly upregulated progenitor genes, we next assessed whether these changes were accompanied by a loss of glial identity. Using microarray analysis, we analyzed a set of MG-specific genes, previously characterized in MG by Ueki et al. (Ueki et al., 2012) (Fig. 6A). These genes are highly enriched in dissociated GFP-infected P12 MG at levels comparable to those in FAC-sorted Hes5– GFP+ MG. Many of these genes, including *Slc1a3*, *Sox9*, *Rlbp1*, *Aqp4* and *Glul*, were downregulated following ASCL1 infection of P12 MG. We confirmed that two of these glial genes, *Rlbp1* (also known as *Cralbp*) and *Slc1a3* (also known as *Glast*), were downregulated by qPCR following ASCL1 infection at 6, 8 and 13 dpi (Fig. 6B). Additionally, immunofluorescence of the glial marker S100β was highly reduced by 4 days after Ascl1 induction (Fig. 6C). We also carried out western blots for two MG-specific proteins, Rlbp1 and GS (Glul), and found that both of these proteins were reduced after ASCL1 infection (Fig. 6D,E).

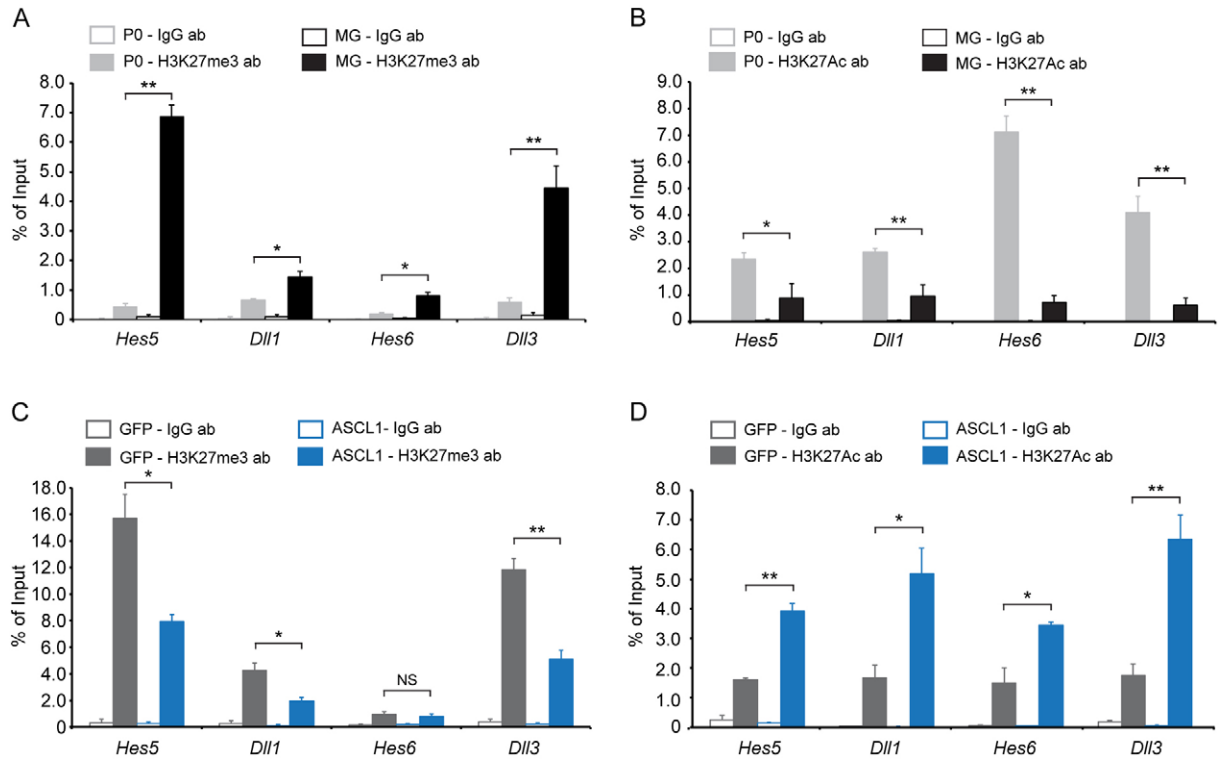

Fig. 5. ASCL1 remodels MG chromatin. ChIP, shown as percentage of input DNA, versus IgG control antibodies at the 5′ promoter of genes indicated. (**A**,**B**) ChIP for H2K27me3 (A) or H2K27Ac (B) in P0 RPCs or MG. (**C**,**D**) ChIP for H3K27me3 (C) or H3K27Ac (D) in ASCL1- or GFP-infected P12 MG at 4 dpi. Data are mean±s.e.m. *P<0.05, **P<0.01; Student's t-test.

ASCL1-reprogrammed MG generate cells with neuronal properties

We next assessed the ASCL1-reprogrammed MG for neuronal properties. By 6 days after ASCL1 infection, these cells had lost their glial morphology and adopted a neuronal appearance. Whereas cultured MG have large, flat cell bodies, neuron-like cells with small, round nuclei and long, thin processes were observed after ASCL1 infection (Fig. 7A).

These morphological changes were associated with robust expression of general neuronal markers. By 6 dpi, ASCL1-infected MG highly expressed the pan-neuronal marker βIII-tubulin (Tubb3; also known as Tuj1) (Fig. 7B). qPCR confirmed that *Tubb3* was significantly enriched in ASCL1-infected MG compared with controls, and that P12 and adult MG upregulated *Tubb3* to similar levels (Fig. 7C). To confirm that these neurons were newly generated from MG, we cultured MG from *Rlbp1*-

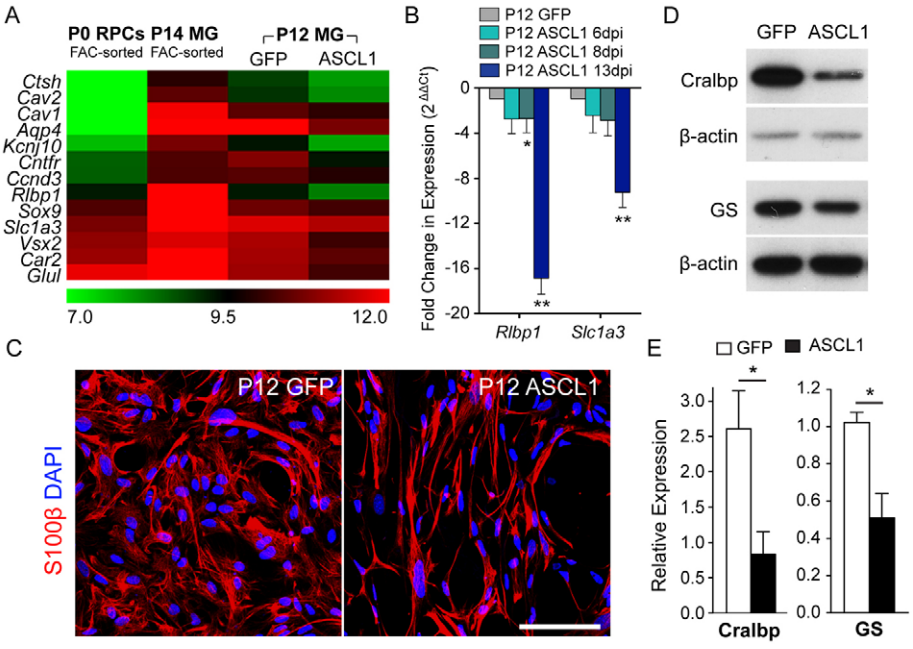

Fig. 6. ASCL1-reprogrammed MG have reduced glial gene expression. (**A**) MG-associated genes in Hes5– GFP+ FAC-sorted P0 progenitors, P14 MG and cultured P12 GFP- or ASCL1-infected MG at 4 dpi. Expression levels are log transformed normalized values. (**B**) qPCR of the MG genes *Rlbp1* (*Cralbp*) and *Slc1a3* (*Glast*) in ASCL1-infected MG compared with GFP-infected MG at 6, 8 and 13 dpi. (**C**) S100β expression is reduced after ASCL1 infection of P12 MG at 4 dpi. (**D**) Western blots of the MG markers Cralbp (Rlbp1) and GS (Glul) after ASCL1 infection at 7 dpi. (**E**) Quantification of western blots normalized to β-actin. Data are mean±s.e.m. *P<0.05, **P<0.01; Student's t-test. Scale bar: 100 μm.

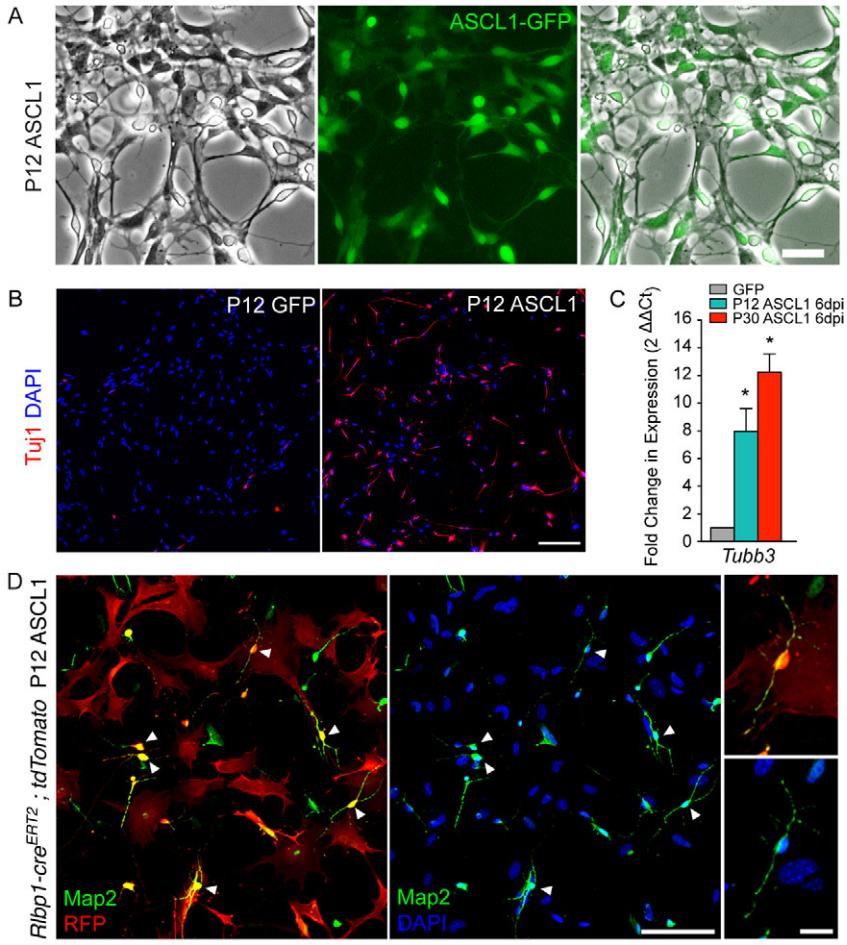

Fig. 7. ASCL1-reprogrammed MG adopt neuronal properties. (**A**) ASCL1-infected MG (native ASCL1-GFP) adopt neuronal morphology (18 dpi). (**B**) The pan-neuronal marker Tuj1 labels ASCL1-infected MG at 10 dpi. (**C**) *Tuj1* mRNA (*Tubb3*) in ASCL1-infected P12 or adult MG at 6 dpi. (**D**) ASCL1-infected P12 MG derived from glial fate mapped *Rlbp1-cre^{ERT2};tdTomato* retinas (RFP+) express Map2 at 10 dpi. Arrowheads indicate double-labeled cells with neuronal appearance. Data are mean±s.e.m. *P<0.05; Student's *t*-test. Scale bars: in A, 50 µm; in B,D, 100 µm; in D, high magnification, 20 µm.

cre^{ERT2};R26-flox-stop-tdTomato P12 retinas (supplementary material Fig. S6A). These mice express cre-recombinase under the control of the MG-specific *Rlbp1* (also known as *Cralbp*) promoter, and, following tamoxifen administration, Cralbp+ MG expressed tdTomato both *in vivo* and in dissociated P12 cultures (supplementary material Fig. S6B,C). Following ASCL1 infection, *Rlbp1-cre^{ERT2};tdTomato*-derived MG adopted neuronal morphology and expressed Map2 (Fig. 7D; Fig. 8A) and Tuj1 (not shown).

In addition to the lineage-tracing experiments, we also followed the progeny of the MG with EdU. The majority of the MG incorporate EdU *in vitro* (Fig. 1), whereas any neurons that survived from the initial retinal dissociation do not. We found that the majority of Tuj1+ and Map2+ cells in the ASCL1-infected MG cultures were EdU+ and were, thus, newly generated from proliferating MG. We quantified the number of EdU+ cells that labeled with these markers and found that >25% expressed Tuj1 or Map2 in ASCL1-infected P12 MG at 9-12 dpi (Fig. 8C). We also found many Tuj1+EdU+ and Map2+EdU+ double-labeled cells in adult MG at 10 dpi (Fig. 8B,D). Thus, progeny of ASCL1-reprogrammed MG can differentiate into cells with neuronal morphology and expression of pan-neuronal markers.

ASCL1-reprogrammed MG express retinal-specific neuronal markers

As ASCL1 can induce pan-neuronal markers and morphology, we investigated whether more specific retinal neuronal genes could be induced in cells derived from ASCL1-infected MG. We analyzed retinal specification genes that are normally expressed after progenitors have exited the cell cycle: *Neurod4*, *Otx2*, *Neurod1*, *Prox1*, *Crx*, *Isl1* and *Atoh7*. All of these early post-mitotic neuronal markers were upregulated by 6 dpi in both P12 and adult MG (Fig. 8E).

These immature retinal neuronal markers were validated further by immunolabeling. Otx2 is a marker of early photoreceptor and bipolar cells (Brzezinski et al., 2010; Omori et al., 2011). Many of the progeny (~30%) of ASCL1-infected MG developed into cells expressing Otx2 (Fig. 8F,I). Another early bipolar marker, Islet 1 (Isl1), was expressed in ASCL1-infected EdU+ MG (Fig. 8G,J), although in a much smaller percentage of the cells. Calretinin (calbindin 2 – Mouse Genome Informatics), a marker of amacrine cells and some bipolar cells, was expressed by ~20% of EdU+ ASCL1-infected MG (Fig. 8H,K). Although the cells appeared to be progressing in their differentiation program, the majority of the differentiating neuronal cells continued to express progenitor markers. Otx2 and Id1 double-labeled cells are shown in Fig. 8L,M, but we also found Hes5 and Sox9 expression in cells labeled with neuronal markers Tuj1 and Map2 (not shown).

We also used qPCR and immunolabeling to determine whether mature retinal neuronal markers were expressed in the progeny of the ASCL1-infected MG. We observed a low, but consistent, level of expression of genes that are normally expressed in mature retinal neurons (supplementary material Fig. S7). The qPCR showed upregulation of *Gad1* (also known as *Gad67*) and *Bhlhe22* (also known as *Bhlhb5*), genes that are normally expressed in mature amacrine and bipolar neurons, respectively. In addition, ASCL1-

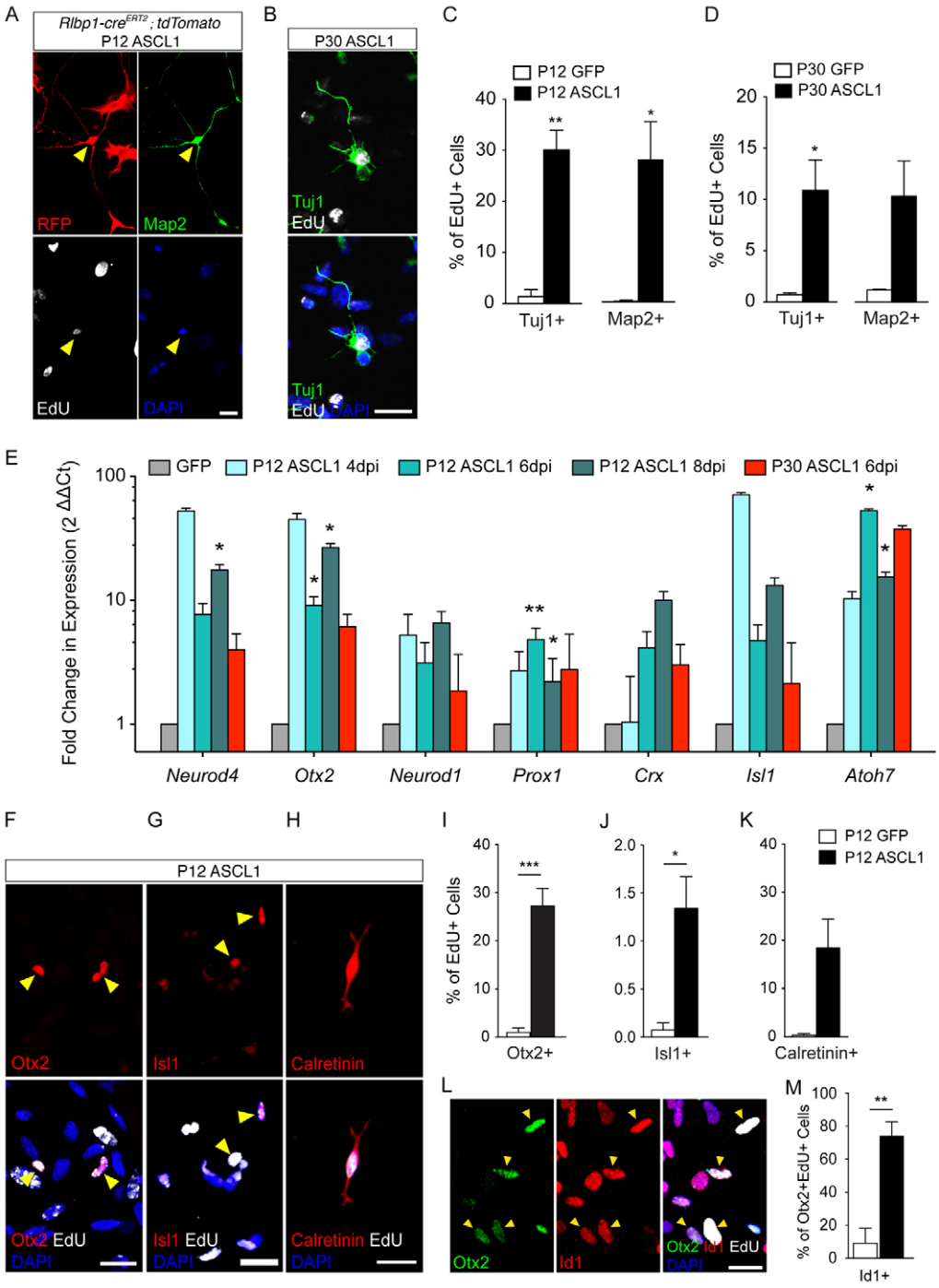

Fig. 8. Retinal-specific neuronal genes are increased in ASCL1-reprogrammed MG. (**A**) ASCL1-infected RFP+ P12 MG from *Rlbp1-cre*^{ERT2}*;tdTomato* retinas co-express Map2 and EdU at 10 dpi. Yellow arrowheads indicate triple-labeled cells. (**B**) Adult EdU+ MG express Tuj1 10 days after ASCL1 infection. (**C**,**D**) Tuj1 and Map2 in ASCL1-infected EdU+ P12 MG at 9-12 dpi (C) and P30 MG at 10 dpi (D). (**E**) qPCR for early neuronal markers in P12 and adult ASCL1- and GFP-infected MG at 4-8 dpi. (**F-H**) EdU+ ASCL1-infected MG express Otx2 (F), Islet1 (G) and calretinin (H). Yellow arrowheads indicate double-labeled cells. (**I-K**) Expression of the retinal neuronal markers Otx2, Isl1 and calretinin in ASCL1-infected EdU+ MG at 9-12 dpi. (**L**) Otx2 and the MG/progenitor marker Id1 are co-expressed in P12 ASCL1-infected MG at 10 dpi. Yellow arrowheads indicate triple-labeled cells. (**M**) The majority of Otx2+EdU+ cells are positive for Id1 in ASCL1-infected MG. Data are mean±s.e.m. **P*<0.05, ***P*<0.01, ****P*<0.001; Student's *t*-test. Scale bars: 20 μm.

infected MG expressed the bipolar markers *Cabp5* and *Vsx1*, and the rod photoreceptor marker *Nrl*. However, the expression levels of most of these genes were very low, and other later-expressed photoreceptor genes, such as *Opn2* (rhodopsin) and *Opn1sw* (also known as S opsin), were not detectable in the reprogrammed MG. These results indicate that ASCL1-reprogrammed MG can develop into cells expressing many early markers of retinal neuronal differentiation; however, a declining percentage expresses later markers and only a very few develop more mature marker expression. Interestingly, the predominant cell type generated in these cultures expresses markers consistent with the bipolar cell fate.

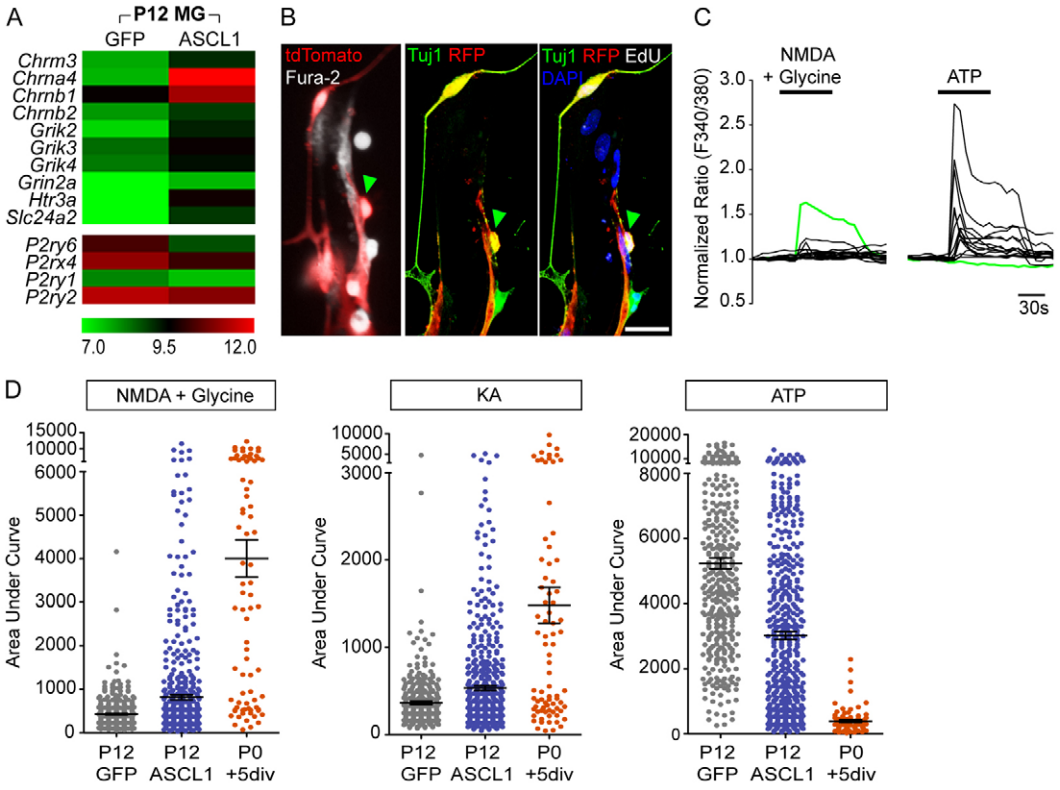

Fig. 9. ASCL1-reprogrammed MG have neuron-like responses to neurotransmitters. (**A**) Microarray analysis of GFP- and ASCL1-infected P12 MG at 4 dpi. The expression levels are log transformed and normalized. (**B**) Example of *Rlbp1-cre^{ERT2};tdTomato* ASCL1-infected P12 MG labeled with Fura-2 Ca^{2+} indicator dye, 10 dpi. Green arrowhead indicates tdTomato+ cell with neuronal morphology postfixed and co-labeled with Tuj1 and EdU. (**C**) Baseline normalized ΔF340/380 responses to NMDA and ATP of cells shown in B. Green traces indicate unique responses from cell marked by arrowheads in B. (**D**) Summary of ΔF340/380 responses, plotted as area under curve, for a 120-second period following application of NMDA (100 μM) + glycine (10 μM), kainate (10 μM), and ATP (100 μM) from one experiment of P12 MG at 10 dpi compared with P0 +5div RPCs. Data are mean±s.e.m. ****P<0.0001; Student's t-test comparing GFP to ASCL1 within each experiment. Similar significance values were found from three biologically independent experiments.

Glial-derived neurons exhibit neuron-like responses to neurotransmitters

To assess whether ASCL1-induced neurons could have functional activity, we looked for gene expression changes in neurotransmitter receptors (Fig. 9A). By 4 dpi, ASCL1-infected MG upregulated many neurotransmitter receptors, the most prevalent of which were nicotinic cholinergic and kainate receptors. At the same time, ASCL1-infected MG downregulated P2Y and P2X purinergic receptors, which are normally highly expressed in MG (Wurm et al., 2009; Wurm et al., 2011).

We next tested whether cells derived from the reprogrammed MG could respond to pharmacological agonists using Ca^{2+} imaging. At 10-12 dpi, cells were loaded with the ratiometric Ca^{2+} indicator dye Fura-2. NMDA (plus glycine to potentiate responses), kainate (KA), ATP and KCl were bath-applied to cells, and ΔF340/380 responses were measured. ASCL1-infected MG were derived from *Rlbp1-cre^{ERT2};tdTomato* retinas; tdTomato+ cells with neuronal morphologies (Fig. 9B, arrowheads) had detectable ΔF340/380 responses to NMDA and failed to respond to ATP, unlike neighboring cells with glial morphology (Fig. 9C). In some cases, we were able to locate the field after fixation, and, in the example shown, the cell was later identified by Tuj1 and EdU immunolabeling (Fig. 9B).

We next assessed overall changes in responsiveness to these agonists in ASCL1- or GFP-infected wild-type MG or retinal neurons from newborn mice (P0, 5-12 div). Figure 9D shows signals, plotted as area under the curve, for individual cells responding to NMDA, KA and ATP. ASCL1 infection caused a significant increase in responsiveness to NMDA and KA and a significant decrease in responsiveness to ATP. These differences were more pronounced in ASCL1-infected MG that had a neuronal or transitional morphology compared with those with a glial morphology or GFP-infected MG (supplementary material Fig. S8B). More modest differences were observed in response to KCl (supplementary material Fig. S8A). Thus, neuronal cells derived from reprogrammed MG responded to ionotropic glutamate agonists but had reduced responsiveness to purinergic receptor agonists. We also confirmed the Ca^{2+} imaging results by whole-cell patch clamp recordings (supplementary material Fig. S9). Injection of 40 pA could elicit action potentials from ASCL1-infected MG cells, application of kainate induced robust inward currents, and when the ASCL1-infected MG were co-cultured with immature retinal neurons, mini-excitatory postsynaptic currents (EPSCs) could be observed.

ASCL1-expressing MG generate new bipolar neurons in retinal explants

To test whether ASCL1 could induce neuronal conversion of MG in the intact retina, *Hes5-GFP* explants, which label MG, were infected with ASCL1. We first validated that MG in P12 *Hes5-GFP*

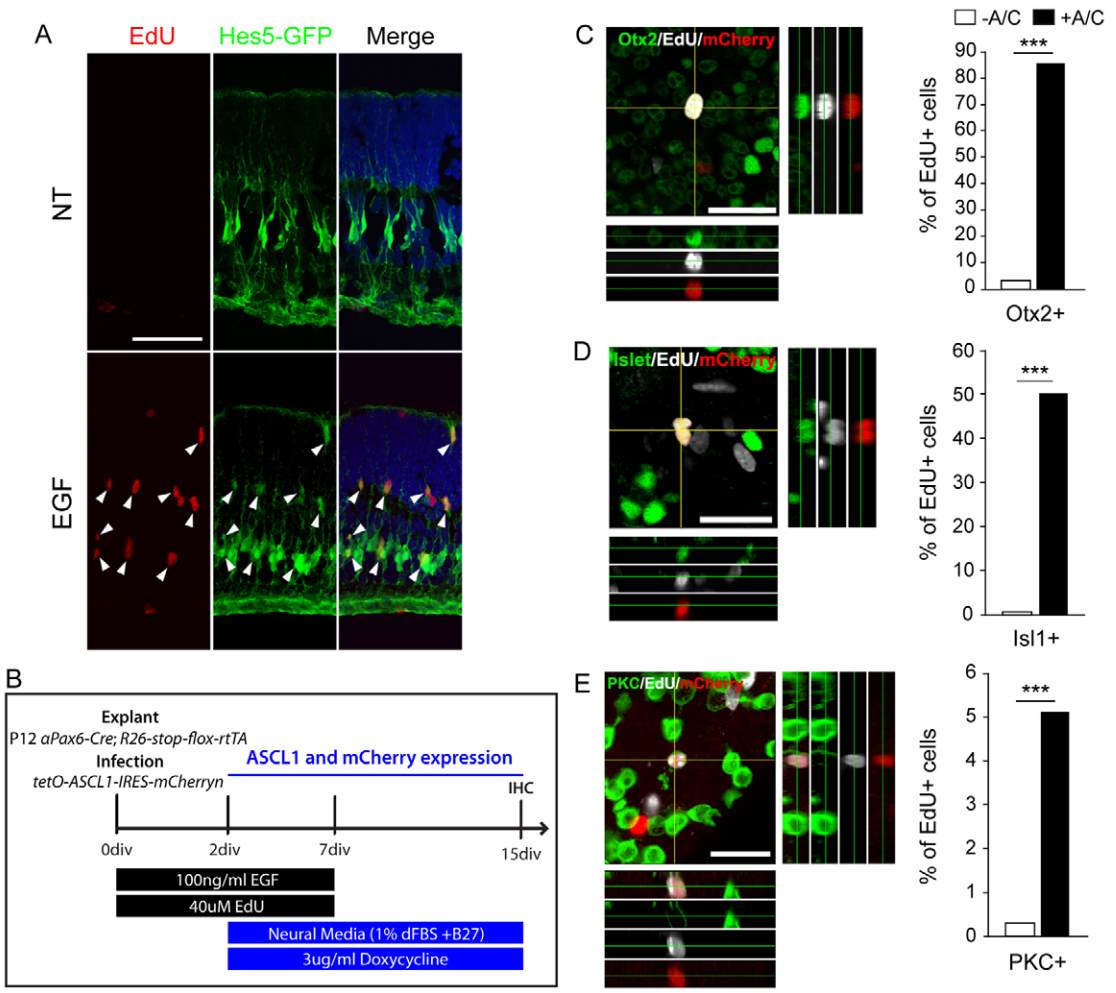

Fig. 10. ASCL1 promotes reprogramming of MG into bipolar cells in retinal explants. (**A**) *Hes5-GFP* retinas explanted at P12 with EdU with or without EGF, 5 div. Proliferating MG are shown (Hes5–GFP+EdU+, arrowheads). NT, non-treated. (**B**) Experimental design. IHC, immunohistochemistry. (**C-E**) EdU+ (MG-derived) mCherry+ cells express Otx2 (C), Islet1 (D) and PKC (E). The percentage EdU+ cells for each marker in ASCL1-infected (+A/C) and uninfected (–A/C) MG are shown on the right. Four to eight random fields per explant, seven explants per marker were analyzed. *Z*-test, ***$P<0.001$; *Z*-score= –17.7 (C), –3.9 (D), –18.9 (E). Scale bars: 50 μm (A); 20 μm (C-E).

retinas cultured as explants re-entered the mitotic cell cycle in response to EGF and incorporated EdU (Fig. 10A) (Ueki et al., 2012), as previous studies in other species suggest that MG have to re-enter the cell cycle prior to their de-differentiation to progenitor cells. MG typically migrate to the outer nuclear layer during regeneration in those species where this process occurs naturally, and we find that the same occurs in the explant cultures of mouse retina when stimulated to proliferate with EGF. To induce ASCL1 expression reliably, we then explanted retinas from α*Pax6-cre;R26-stop-flox-rtTA* P12 mice, resulting in reverse tetracycline transactivator (rtTA) expression in the peripheral retina (Fig. 10B). EGF was added to promote MG proliferation, and EdU was included to track MG and their progeny. Explants were infected with *tetO-ASCL1-mCherryn* lentivirus in neural medium, and doxycycline was added after two days to activate ASCL1 and mCherry expression. ASCL1 and mCherry nearly perfectly colocalized in HEK293T cells as well as in explants (supplementary material Fig. S10); therefore, mCherry was used as a reliable marker for ASCL1-expressing cells.

Thirteen days after the induction of ASCL1-mCherry, retinal explants were immunolabeled with neuronal markers. Similar to what was observed in dissociated ASCL1-infected MG cultures, there were significant numbers of EdU+mCherry+ cells (ASCL1-infected MG) that expressed bipolar cell markers (Fig. 10C-E). Over 80% of ASCL1-infected MG (EdU+mCherry+) expressed Otx2 compared with <5% of uninfected cells (EdU+mCherry–) (Fig. 10C). Approximately half of the ASCL1-expressing proliferating MG progeny also expressed Islet 1, compared with <1% of the uninfected, EdU+mCherry– population (Fig. 10D). ASCL1-infected MG also expressed protein kinase C (PKC), a marker of more mature bipolar cells. Approximately 5% of ASCL1-infected MG (EdU+mCherry+) expressed PKC compared with <1% of uninfected MG (EdU+mCherry–) (Fig. 10E). Many of the MG-derived cells that expressed bipolar markers were in the inner nuclear layer, with the existing bipolar cells, though some were also located ectopically in the outer nuclear layer. No significant cell death was observed by DAPI staining (data not shown), suggesting that newborn cells survive in the native environment.

DISCUSSION

Here, we report that mammalian MG can be reprogramed to a neurogenic state by forced expression of the proneural transcription

factor ASCL1. ASCL1 remodeled repressive chromatin at its targets to an active state and induced expression of progenitor genes, while downregulating MG genes. Reprogrammed MG produced cells that express pan-neuronal markers, exhibit neuronal morphology and upregulate many retinal-specific neuronal markers. Furthermore, the MG-derived ASCL1-induced neurons exhibited functional activity in response to appropriate neurotransmitter receptor agonists. Finally, ASCL1-reprogramming of MG in the intact retina revealed that newly generated neurons primarily differentiated as bipolar cells that integrated within the pre-existing neuronal population.

ASCL1 was sufficient to induce the re-expression of many progenitor genes, while inhibiting the glial differentiation program. Direct targets of Ascl1, *Dll1*, *Dll3*, *Hes5*, *Hes6* and *Mfng* (Ueno et al., 2012; Castro et al., 2011), were bound and re-activated in the MG, and progenitor genes that are not direct Ascl1 targets, such as *Neurog2* and *Mycn*, were also increased; moreover, the Ascl1 promoter was partly remodeled to a more active state. Taken together, these results suggest that ASCL1 initiates extensive reprogramming of the MG.

The response of mouse MG to ASCL1 expression is reminiscent of observations in zebrafish after retinal damage, in which MG de-differentiate into progenitors after upregulating *ascl1a* (Fausett et al., 2008; Ramachandran et al., 2010; Thummel et al., 2008; Raymond et al., 2006). We observed that ASCL1 overexpression upregulates Notch pathway components and Insm1, which are downstream of Ascl1a and required for de-differentiation in the regenerating fish retina (Ramachandran et al., 2012; Wan et al., 2012).

ASCL1 appears to reprogram MG through a transitional progenitor state, and stimulates proliferation; however, we cannot say whether this is an obligatory step in the process of reprogramming MG, as we did not determine whether the neuronal cells derived from the MG have undergone a mitotic division after infection; moreover, direct neuronal reprogramming of astrocytes (Heinrich et al., 2010) to neurons with Neurog2 does not require mitotic division.

The reprogramming of MG by ASCL1 includes remodeling of the chromatin at the promoters of progenitor genes, including *Ascl1* itself, for at least two important histone modifications. During glial differentiation, progenitors acquire the repressive chromatin mark H3K27me3 and lose the activation mark H3K27Ac at Ascl1 and its targets. However, at targets where Ascl1 was bound by ChIP, ASCL1-expressing MG lost this repressive mark and gained the activation mark (although it is difficult to compare quantitatively the epigenetic state of these chromatin modifications between the progenitors and the reprogrammed MG owing to heterogeneity in the populations). Several models have been put forth to explain reprogramming in contexts in which transcription factors are forcibly expressed (Vierbuchen and Wernig, 2012). One model suggests a ‘permissive enhancer’, i.e. a transcription factor is able to bind at sites of open chromatin at enhancers of activatable genes (Taberlay et al., 2011). An alternative model suggests that these factors can act as ‘pioneers’ and bind repressed elements to pave the way for other factors (Zaret and Carroll, 2011; Cao et al., 2010).

MG-derived progenitor-like cells differentiated to form cells that shared morphological, immunohistochemical and functional characteristics with retinal neurons. ASCL1-reprogrammed cells adopted a distinctly neuronal appearance by 6 dpi, which coincided with their expression of pan-neuronal markers. These cells were responsive to ionotropic glutamate agonists, NMDA and kainate, and showed decreased responsiveness to the purinergic receptor agonist ATP. These effects are comparable to those from studies of neurogenic reprogramming in postnatal cortical astrocytes (Addis et al., 2011; Berninger et al., 2007; Blum et al., 2011; Corti et al., 2012; Heinrich et al., 2010; Heins et al., 2002) and pericytes (Karow et al., 2012). Berninger et al. (Berninger et al., 2007) and Heinrich et al. (Heinrich et al., 2010) found that Ascl1 or Neurog2 expression could convert fate-mapped postnatal astrocytes into morphologically distinct neurons by 4 dpi. However, astrocyte-derived neurons did not form synapses and mature membrane properties until 2-3 weeks *in vitro*, suggesting that maturation may take significantly longer than initial reprogramming and cell-type specification.

Newly generated neuronal cells from ASCL1-reprogrammed MG primarily differentiated as bipolar cells. In dissociated MG, ASCL1 induced early markers of many retinal neuron subtypes; however, later neuronal markers were more restricted to bipolar cells (Otx2, Islet 1, calretinin, Vsx1, Cabp5, Bhlhb5 and PKC) and, possibly, amacrine cells (Gad67, Bhlhb5, calretinin). The bias towards bipolar cells was also apparent in retinal explants, in which ASCL1-infected MG generated a large number of Otx2+ and Islet 1+ cells and a smaller number of PKC+ rod bipolar cells. This is consistent with the role of Ascl1 during normal development, as Ascl1 is expressed in late progenitors, which give rise to amacrine cells, bipolar cells and photoreceptors, but not ganglion cells (Brzezinski et al., 2011), and deletion of *Ascl1* in mice leads to a reduction in bipolar cells and photoreceptors (Akagi et al., 2004; Tomita et al., 2000; Brzezinski et al., 2011).

Previous reports have suggested that dissociated MG, from both mouse and human, can act as stem cells by self-renewing and differentiating towards multiple neural lineages (Das et al., 2006; Nickerson et al., 2008; Lawrence et al., 2007; Giannelli et al., 2010). However, many of the stem and progenitor markers used in these studies, such as nestin and Sox2, are expressed in cultured MG (Karl et al., 2008; Bhatia et al., 2011; Lin et al., 2009), and they are not sufficient to specify the neural stem/progenitor fate. Recently, reports have suggested that MG spontaneously produce neurons *in vitro* (Giannelli et al., 2010) or when co-cultured with hippocampal explants (Das et al., 2006). However, neither experiment distinguished putative new neurons from those that survived the dissociation (e.g. using a thymidine analog or lineage-tracing method). Significant numbers of neurons can survive in dissociated retinal cell cultures, even after passage, and thus a method to distinguish surviving neurons from newly generated ones is crucial.

Additionally, reports have claimed that MG in mouse and rat retina can regenerate new neurons after damage if treated with exogenous factors. Wnt3a, EGF, fibroblast growth factor (FGF), insulin-like growth factor (IGF), retinoic acid (RA), Notch, N-methyl-N-nitrosourea (MNU) and α-aminoadipic acid (α-AA) have all been shown to stimulate a small number of MG to re-enter the mitotic cell cycle (Ooto et al., 2004; Close et al., 2006; Osakada et al., 2007; Wan et al., 2008; Takeda et al., 2008; Karl et al., 2008; Del Debbio et al., 2010). Some of the progeny of the bromodeoxyuridine (BrdU)+ MG were reported to differentiate characteristics of various types of retinal neurons, depending on the study and the treatment. However, only one of these studies used confocal imaging and 3D reconstruction to characterize definitively the BrdU+ cells (Karl et al., 2008), and that study was only able to find a small number of new amacrine cells generated from the BrdU+ MG (3.6%).

It is unclear why ASCL1-reprogrammed neurons do not more efficiently differentiate and mature. ASCL1 alone was sufficient to activate pan-neuronal and early markers of retinal neurons robustly, but we found lower levels of genes expressed by more mature retinal neurons, such as rhodopsin and S opsin. ASCL1 can activate

its direct targets, including *Otx2*, which commits progenitors to photoreceptor or bipolar fates. However, direct targets of Otx2, such as *Nrl* and *Pde6b*, are not robustly expressed, and only 5% of ASCL1-infected MG differentiated to PKC+ bipolar cells, although much higher percentages expressed Otx2 and Isl1. Several potential mechanisms could account for the limited ability of MG-derived neurons to mature fully. Continued expression of progenitor markers, such as Sox9, Id1 and Hes5, may limit full differentiation, though this might also be due to continued expression of ASCL1 in the cells. It may also be the case that factors in the retinal environment, not present in the dissociated cultures, are needed for differentiation and/or survival of the new neurons derived from the ASCL1-reprogrammed MG. Evidence for this comes from the fact that a much higher percentage of the ASCL1-reprogrammed MG express Otx2 and Isl1 in the explant cultures than in the dissociated cell cultures. Epigenetic restrictions in the MG might also limit full reprogramming. Although repressive histone modifications are remodeled at the Ascl1 targets, other genes might persist in a repressed state. Genes required in photoreceptors, e.g. rhodopsin, might be repressed by different mechanisms than are progenitor and early neuronal specification genes. A recent report by Powell et al. (Powell et al., 2012) found that retinal regeneration in fish required expression of the cytidine deaminases *apobec2a* and *apobec2b*, which are involved in DNA demethylation.

Viral overexpression of ASCL1 in MG suggests a strategy for stimulating regeneration of the mammalian retina. This approach is complementary to transplantation of stem cell-derived neurons for retinal repair, as it allows for MG to be targeted for reprogramming within their native environment. Viral reprogramming of MG cells with ASCL1 predominantly generates bipolar neurons, so other reprogramming factors will probably be needed to direct the MG to photoreceptors and ganglion cells. Nevertheless, our study shows that viral reprogramming may allow MG to serve as a source of new retinal neurons to treat retinal degenerative diseases and one day provide a basis for gene therapeutic approaches.

Acknowledgements
We thank Drs Olivia Bermingham-McDonogh, Rachel Wong and Anna La Torre for helpful manuscript comments; Kristin Sternhagen for cloning expertise; and Ajay Dhaka for help with Ca^{2+} imaging experiments.

Funding
This work was supported by grants from the National Institutes of Health [1R01EY021482 to T.A.R.; R01-EY013760 to E.M.L.]; a Developmental Biology Predoctoral Training Grant from the National Institute of Child Health and Human Development [T32HD007183 to J.P.]; a National Science Foundation Fellowship [DGE-0718124 to M.S.W.]; and a Vision Core Grant [P30EY01730]. Deposited in PMC for release after 12 months.

Competing interests statement
The authors declare no competing financial interests.

Supplementary material
Supplementary material available online at
http://dev.biologists.org/lookup/suppl/doi:10.1242/dev.091355/-/DC1

References

Addis, R. C., Hsu, F.-C., Wright, R. L., Dichter, M. A., Coulter, D. A. and Gearhart, J. D. (2011). Efficient conversion of astrocytes to functional midbrain dopaminergic neurons using a single polycistronic vector. *PLoS ONE* **6**, e28719.

Akagi, T., Inoue, T., Miyoshi, G., Bessho, Y., Takahashi, M., Lee, J. E., Guillemot, F. and Kageyama, R. (2004). Requirement of multiple basic helix-loop-helix genes for retinal neuronal subtype specification. *J. Biol. Chem.* **279**, 28492-28498.

Basak, O. and Taylor, V. (2007). Identification of self-replicating multipotent progenitors in the embryonic nervous system by high Notch activity and Hes5 expression. *Eur. J. Neurosci.* **25**, 1006-1022.

Belteki, G., Haigh, J., Kabacs, N., Haigh, K., Sison, K., Costantini, F., Whitsett, J., Quaggin, S. E. and Nagy, A. (2005). Conditional and inducible transgene expression in mice through the combinatorial use of Cre-mediated recombination and tetracycline induction. *Nucleic Acids Res.* **33**, e51.

Bernardos, R. L., Barthel, L. K., Meyers, J. R. and Raymond, P. A. (2007). Late-stage neuronal progenitors in the retina are radial Müller glia that function as retinal stem cells. *J. Neurosci.* **27**, 7028-7040.

Berninger, B. (2010). Making neurons from mature glia: a far-fetched dream? *Neuropharmacology* **58**, 894-902.

Berninger, B., Costa, M. R., Koch, U., Schroeder, T., Sutor, B., Grothe, B. and Götz, M. (2007). Functional properties of neurons derived from in vitro reprogrammed postnatal astroglia. *J. Neurosci.* **27**, 8654-8664.

Bhatia, B., Jayaram, H., Singhal, S., Jones, M. F. and Limb, G. A. (2011). Differences between the neurogenic and proliferative abilities of Müller glia with stem cell characteristics and the ciliary epithelium from the adult human eye. *Exp. Eye Res.* **93**, 852-861.

Blum, R., Heinrich, C., Sánchez, R., Lepier, A., Gundelfinger, E. D., Berninger, B. and Götz, M. (2011). Neuronal network formation from reprogrammed early postnatal rat cortical glial cells. *Cereb. Cortex* **21**, 413-424.

Boyer, L. A., Plath, K., Zeitlinger, J., Brambrink, T., Medeiros, L. A., Lee, T. I., Levine, S. S., Wernig, M., Tajonar, A., Ray, M. K. et al. (2006). Polycomb complexes repress developmental regulators in murine embryonic stem cells. *Nature* **441**, 349-353.

Bringmann, A., Iandiev, I., Pannicke, T., Wurm, A., Hollborn, M., Wiedemann, P., Osborne, N. N. and Reichenbach, A. (2009). Cellular signaling and factors involved in Müller cell gliosis: neuroprotective and detrimental effects. *Prog. Retin. Eye Res.* **28**, 423-451.

Brzezinski, J. A., 4th, Lamba, D. A. and Reh, T. A. (2010). Blimp1 controls photoreceptor versus bipolar cell fate choice during retinal development. *Development* **137**, 619-629.

Brzezinski, J. A., 4th, Kim, E. J., Johnson, J. E. and Reh, T. A. (2011). Ascl1 expression defines a subpopulation of lineage-restricted progenitors in the mammalian retina. *Development* **138**, 3519-3531.

Cao, R., Wang, L., Wang, H., Xia, L., Erdjument-Bromage, H., Tempst, P., Jones, R. S. and Zhang, Y. (2002). Role of histone H3 lysine 27 methylation in Polycomb-group silencing. *Science* **298**, 1039-1043.

Cao, Y., Yao, Z., Sarkar, D., Lawrence, M., Sanchez, G. J., Parker, M. H., MacQuarrie, K. L., Davison, J., Morgan, M. T., Ruzzo, W. L. et al. (2010). Genome-wide MyoD binding in skeletal muscle cells: a potential for broad cellular reprogramming. *Dev. Cell* **18**, 662-674.

Castro, D. S., Skowronska-Krawczyk, D., Armant, O., Donaldson, I. J., Parras, C., Hunt, C., Critchley, J. A., Nguyen, L., Gossler, A., Göttgens, B. et al. (2006). Proneural bHLH and Brn proteins coregulate a neurogenic program through cooperative binding to a conserved DNA motif. *Dev. Cell* **11**, 831-844.

Castro, D. S., Martynoga, B., Parras, C., Ramesh, V., Pacary, E., Johnston, C., Drechsel, D., Lebel-Potter, M., Garcia, L. G., Hunt, C. et al. (2011). A novel function of the proneural factor Ascl1 in progenitor proliferation identified by genome-wide characterization of its targets. *Genes Dev.* **25**, 930-945.

Close, J. L., Liu, J., Gumuscu, B. and Reh, T. A. (2006). Epidermal growth factor receptor expression regulates proliferation in the postnatal rat retina. *Glia* **54**, 94-104.

Corti, S., Nizzardo, M., Simone, C., Falcone, M., Donadoni, C., Salani, S., Rizzo, F., Nardini, M., Riboldi, G., Magri, F. et al. (2012). Direct reprogramming of human astrocytes into neural stem cells and neurons. *Exp. Cell Res.* **318**, 1528-1541.

Das, A. V., Mallya, K. B., Zhao, X., Ahmad, F., Bhattacharya, S., Thoreson, W. B., Hegde, G. V. and Ahmad, I. (2006). Neural stem cell properties of Müller glia in the mammalian retina: regulation by Notch and Wnt signaling. *Dev. Biol.* **299**, 283-302.

Del Debbio, C. B., Balasubramanian, S., Parameswaran, S., Chaudhuri, A., Qiu, F. and Ahmad, I. (2010). Notch and Wnt signaling mediated rod photoreceptor regeneration by Müller cells in adult mammalian retina. *PLoS ONE* **5**, e12425.

Dyer, M. A. and Cepko, C. L. (2000). Control of Müller glial cell proliferation and activation following retinal injury. *Nat. Neurosci.* **3**, 873-880.

Eden, E., Lipson, D., Yogev, S. and Yakhini, Z. (2007). Discovering motifs in ranked lists of DNA sequences. *PLoS Comput. Biol.* **3**, e39.

Eden, E., Navon, R., Steinfeld, I., Lipson, D., and Yakhini, Z. (2009). GOrilla: a tool for discovery and visualization of enriched go terms in ranked gene lists. *BMC Bioinformatics* **3**, 10-48.

Fausett, B. V., Gumerson, J. D. and Goldman, D. (2008). The proneural basic helix-loop-helix gene ascl1a is required for retina regeneration. *J. Neurosci.* **28**, 1109-1117.

Gamm, D. M., Wright, L. S., Capowski, E. E., Shearer, R. L., Meyer, J. S., Kim, H.-J., Schneider, B. L., Melvan, J. N. and Svendsen, C. N. (2008). Regulation of prenatal human retinal neurosphere growth and cell fate potential by retinal pigment epithelium and Mash1. *Stem Cells* **26**, 3182-3193.

Giannelli, S. G., Demontis, G. C., Pertile, G., Rama, P. and Broccoli, V. (2010). Adult human Müller glia cells are a highly efficient source of rod photoreceptors. *Stem Cells* **29**, 344-356.

Hatakeyama, J., Tomita, K., Inoue, T. and Kageyama, R. (2001). Roles of homeobox and bHLH genes in specification of a retinal cell type. *Development* **128**, 1313-1322.
Heinrich, C., Blum, R., Gascón, S., Masserdotti, G., Tripathi, P., Sánchez, R., Tiedt, S., Schroeder, T., Götz, M. and Berninger, B. (2010). Directing astroglia from the cerebral cortex into subtype specific functional neurons. *PLoS Biol.* **8**, e1000373.
Heins, N., Malatesta, P., Cecconi, F., Nakafuku, M., Tucker, K. L., Hack, M. A., Chapouton, P., Barde, Y. A. and Götz, M. (2002). Glial cells generate neurons: the role of the transcription factor Pax6. *Nat. Neurosci.* **5**, 308-315.
Jasoni, C. L. and Reh, T. A. (1996). Temporal and spatial pattern of MASH-1 expression in the developing rat retina demonstrates progenitor cell heterogeneity. *J. Comp. Neurol.* **369**, 319-327.
Karl, M. O., Hayes, S., Nelson, B. R., Tan, K., Buckingham, B. and Reh, T. A. (2008). Stimulation of neural regeneration in the mouse retina. *Proc. Natl. Acad. Sci. USA* **105**, 19508-19513.
Karlić, R., Chung, H. R., Lasserre, J., Vlahoviček, K. and Vingron, M. (2010). Histone modification levels are predictive for gene expression. *Proc. Natl. Acad. Sci. USA* **107**, 2926-2931.
Karow, M., Sánchez, R., Schichor, C., Masserdotti, G., Ortega, F., Heinrich, C., Gascón, S., Khan, M. A., Lie, D. C., Dellavalle, A. et al. (2012). Reprogramming of pericyte-derived cells of the adult human brain into induced neuronal cells. *Cell Stem Cell* **11**, 471-476.
Lawrence, J. M., Singhal, S., Bhatia, B., Keegan, D. J., Reh, T. A., Luthert, P. J., Khaw, P. T. and Limb, G. A. (2007). MIO-M1 cells and similar muller glial cell lines derived from adult human retina exhibit neural stem cell characteristics. *Stem Cells* **25**, 2033-2043.
Lin, Y. P., Ouchi, Y., Satoh, S. and Watanabe, S. (2009). Sox2 plays a role in the induction of amacrine and Müller glial cells in mouse retinal progenitor cells. *Invest. Ophthalmol. Vis. Sci.* **50**, 68-74.
Mao, W., Yan, R.-T. and Wang, S.-Z. (2008). Reprogramming chick RPE progeny cells to differentiate towards retinal neurons by ash1. *Mol. Vis.* **14**, 2309-2320.
Marquardt, T., Ashery-Padan, R., Andrejewski, N., Scardigli, R., Guillemot, F. and Gruss, P. (2001). Pax6 is required for the multipotent state of retinal progenitor cells. *Cell* **105**, 43-55.
Nelson, B. R., Hartman, B. H., Georgi, S. A., Lan, M. S. and Reh, T. A. (2007). Transient inactivation of Notch signaling synchronizes differentiation of neural progenitor cells. *Dev. Biol.* **304**, 479-498.
Nelson, B. R., Hartman, B. H., Ray, C. A., Hayashi, T., Bermingham-McDonogh, O. and Reh, T. A. (2009). Acheate-scute like 1 (Ascl1) is required for normal delta-like (Dll) gene expression and notch signaling during retinal development. *Dev. Dyn.* **238**, 2163-2178.
Nelson, B. R., Ueki, Y., Reardon, S., Karl, M. O., Georgi, S., Hartman, B. H., Lamba, D. A. and Reh, T. A. (2011). Genome-wide analysis of Müller glial differentiation reveals a requirement for Notch signaling in postmitotic cells to maintain the glial fate. *PLoS ONE* **6**, e22817.
Nickerson, P. E. B., Da Silva, N., Myers, T., Stevens, K. and Clarke, D. B. (2008). Neural progenitor potential in cultured Müller glia: effects of passaging and exogenous growth factor exposure. *Brain Res.* **1230**, 1-12.
Omori, Y., Katoh, K., Sato, S., Muranishi, Y., Chaya, T., Onishi, A., Minami, T., Fujikado, T. and Furukawa, T. (2011). Analysis of transcriptional regulatory pathways of photoreceptor genes by expression profiling of the Otx2-deficient retina. *PLoS ONE* **6**, e19685.
Ooto, S., Akagi, T., Kageyama, R., Akita, J., Mandai, M., Honda, Y. and Takahashi, M. (2004). Potential for neural regeneration after neurotoxic injury in the adult mammalian retina. *Proc. Natl. Acad. Sci. USA* **101**, 13654-13659.
Osakada, F., Ooto, S., Akagi, T., Mandai, M., Akaike, A. and Takahashi, M. (2007). Wnt signaling promotes regeneration in the retina of adult mammals. *J. Neurosci.* **27**, 4210-4219.
Powell, C., Elsaeidi, F. and Goldman, D. (2012). Injury-dependent Müller glia and ganglion cell reprogramming during tissue regeneration requires Apobec2a and Apobec2b. *J. Neurosci.* **32**, 1096-1109.
Ramachandran, R., Fausett, B. V. and Goldman, D. (2010). Ascl1a regulates Müller glia dedifferentiation and retinal regeneration through a Lin-28-dependent, let-7 microRNA signalling pathway. *Nat. Cell Biol.* **12**, 1101-1107.
Ramachandran, R., Zhao, X.-F. and Goldman, D. (2012). Insm1a-mediated gene repression is essential for the formation and differentiation of Müller glia-derived progenitors in the injured retina. *Nat. Cell Biol.* **14**, 1013-1023.
Raymond, P. A., Barthel, L. K., Bernardos, R. L. and Perkowski, J. J. (2006). Molecular characterization of retinal stem cells and their niches in adult zebrafish. *BMC Dev. Biol.* **6**, 36.
Taberlay, P. C., Kelly, T. K., Liu, C.-C., You, J. S., De Carvalho, D. D., Miranda, T. B., Zhou, X. J., Liang, G. and Jones, P. A. (2011). Polycomb-repressed genes have permissive enhancers that initiate reprogramming. *Cell* **147**, 1283-1294.
Takeda, M., Takamiya, A., Jiao, J.-W., Cho, K.-S., Trevino, S. G., Matsuda, T. and Chen, D. F. (2008). alpha-Aminoadipate induces progenitor cell properties of Müller glia in adult mice. *Invest. Ophthalmol. Vis. Sci.* **49**, 1142-1150.
Thummel, R., Kassen, S. C., Enright, J. M., Nelson, C. M., Montgomery, J. E. and Hyde, D. R. (2008). Characterization of Müller glia and neuronal progenitors during adult zebrafish retinal regeneration. *Exp. Eye Res.* **87**, 433-444.
Tomita, K., Moriyoshi, K., Nakanishi, S., Guillemot, F. and Kageyama, R. (2000). Mammalian achaete-scute and atonal homologs regulate neuronal versus glial fate determination in the central nervous system. *EMBO J.* **19**, 5460-5472.
Ueki, Y., Karl, M. O., Sudar, S., Pollak, J., Taylor, R. J., Loeffler, K., Wilken, M. S., Reardon, S. and Reh, T. A. (2012). P53 is required for the developmental restriction in Müller glial proliferation in mouse retina. *Glia* **60**, 1579-1589.
Ueno, T., Ito, J., Hoshikawa, S., Ohori, Y., Fujiwara, S., Yamamoto, S., Ohtsuka, T., Kageyama, R., Akai, M., Nakamura, K. et al. (2012). The identification of transcriptional targets of Ascl1 in oligodendrocyte development. *Glia* **60**, 1495-1505.
Vázquez-Chona, F. R., Clark, A. M. and Levine, E. M. (2009). Rlbp1 promoter drives robust Müller glial GFP expression in transgenic mice. *Invest. Ophthalmol. Vis. Sci.* **50**, 3996-4003.
Vierbuchen, T. and Wernig, M. (2011). Direct lineage conversions: unnatural but useful? *Nat. Biotechnol.* **29**, 892-907.
Vierbuchen, T. and Wernig, M. (2012). Molecular roadblocks for cellular reprogramming. *Mol. Cell* **47**, 827-838.
Vierbuchen, T., Ostermeier, A., Pang, Z. P., Kokubu, Y., Südhof, T. C. and Wernig, M. (2010). Direct conversion of fibroblasts to functional neurons by defined factors. *Nature* **463**, 1035-1041.
Wan, J., Zheng, H., Chen, Z.-L., Xiao, H.-L., Shen, Z.-J. and Zhou, G.-M. (2008). Preferential regeneration of photoreceptor from Müller glia after retinal degeneration in adult rat. *Vision Res.* **48**, 223-234.
Wan, J., Ramachandran, R. and Goldman, D. (2012). HB-EGF is necessary and sufficient for Müller glia dedifferentiation and retina regeneration. *Dev. Cell* **22**, 334-347.
Wurm, A., Erdmann, I., Bringmann, A., Reichenbach, A. and Pannicke, T. (2009). Expression and function of P2Y receptors on Müller cells of the postnatal rat retina. *Glia* **57**, 1680-1690.
Wurm, A., Pannicke, T., Iandiev, I., Francke, M., Hollborn, M., Wiedemann, P., Reichenbach, A., Osborne, N. N. and Bringmann, A. (2011). Purinergic signaling involved in Müller cell function in the mammalian retina. *Prog. Retin. Eye Res.* **30**, 324-342.
Yuan, J. S., Reed, A., Chen, F. and Stewart, C. N., Jr (2006). Statistical analysis of real-time PCR data. *BMC Bioinformatics* **7**, 85.
Zaret, K. S. and Carroll, J. S. (2011). Pioneer transcription factors: establishing competence for gene expression. *Genes Dev.* **25**, 2227-2241.

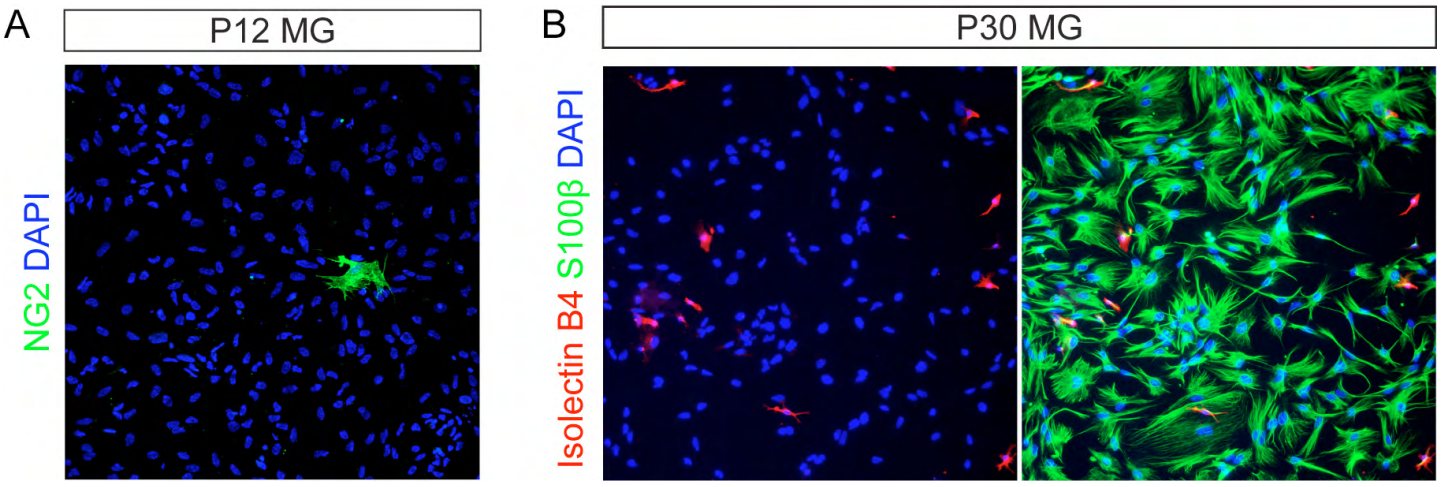

Fig. S1. P12 and P30 MG cultures have low contamination of other cell types. Related to Figs 1, 2. (**A**) Less than 1% of P12 MG labeled with the pericyte marker NG2 after 1 week in culture. (**B**) NMDA-damaged P30 retinas were dissociated 2 days after damage and cultured for one week. The majority of cells label with glial marker S100β, and few cells express the endothelial marker isolectin B4.

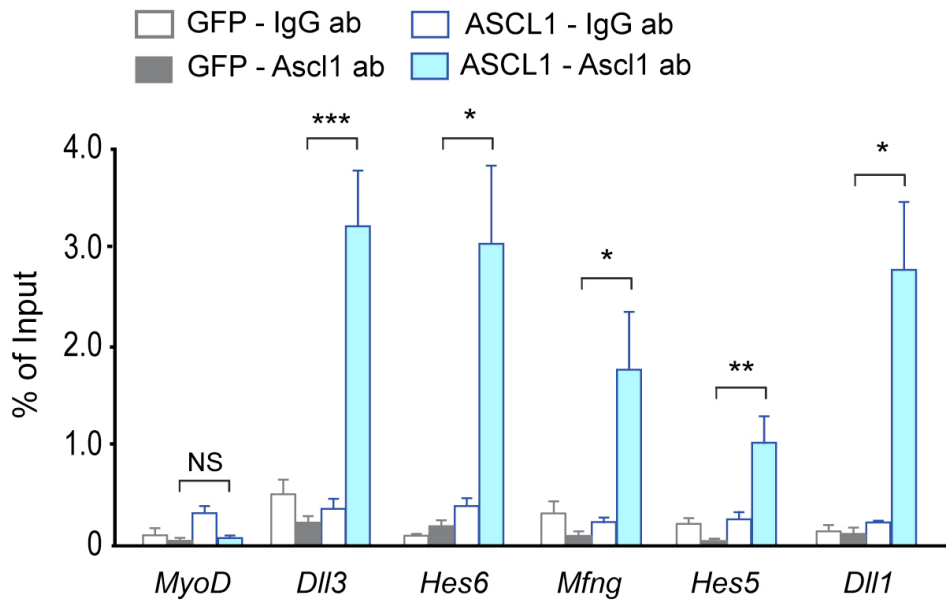

Fig. S2. ASCL1 does not bind predicted targets in GFP-infected MG. Related to Fig. 2. ChIP for Ascl1 or control IgG antibodies at the 5′ promoter region of genes indicated. Significant enrichment of Ascl1 in ASCL1-infected P12 MG compared with GFP-infected P12 MG was observed. Data are mean ± s.e.m. **P*<0.05, ***P*<0.01, ****P*<0.001 by Student's *t*-test.

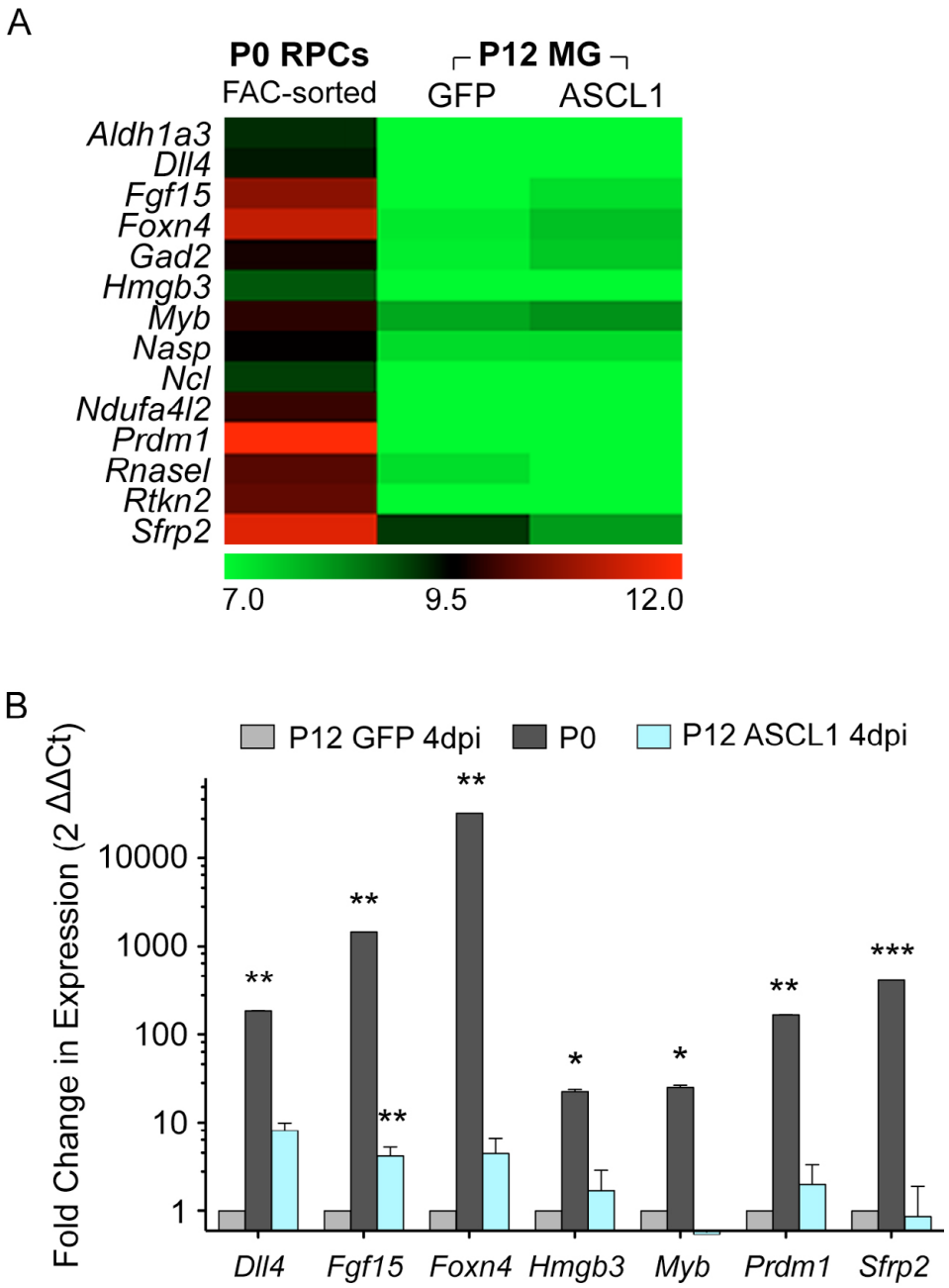

Fig. S3. A subset of progenitor-specific genes are not reactivated in MG by ASCL1 alone. Related to Fig. 2. (**A**) A subset of genes on microarray analysis at 4 dpi are highly expressed (log transformed normalized values) in P0 progenitors but do not upregulate after ASCL1 infection of MG. (**B**) Expression patterns were confirmed by qPCR. Data are mean ± s.e.m. **P*<0.05, ***P*<0.01, ****P*<0.001 by Student's *t*-test.

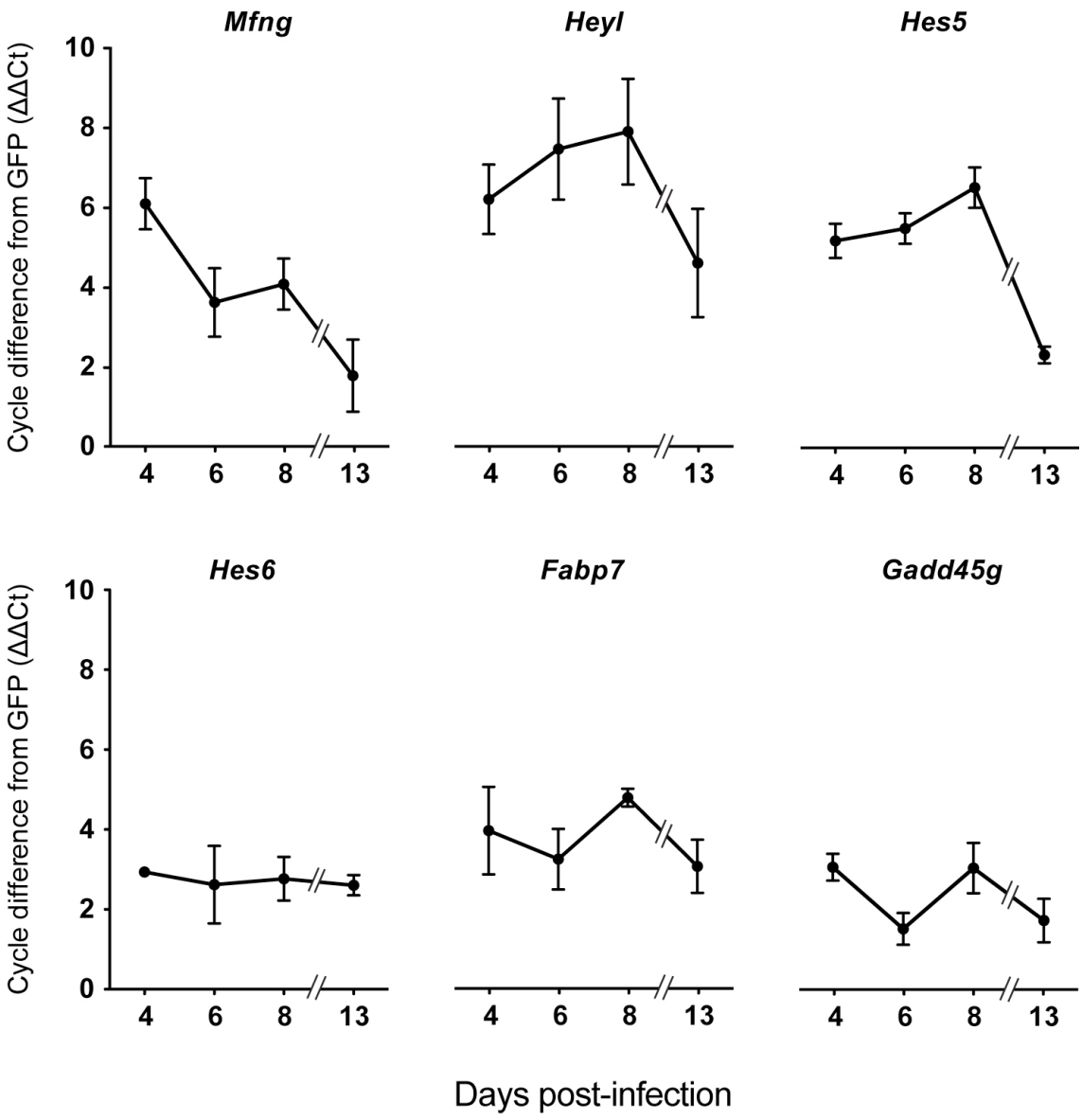

Fig. S4. Timecourse of expression of retinal progenitor genes. Related to Fig. 2. Progenitor genes are enriched in P12 ASCL1-infected MG at 4, 6 and 8 dpi compared with GFP-infected controls from paired data. By 13 dpi, *Mfng*, *Heyl* and *Hes5* are greatly decreased. Data are mean ± s.e.m.

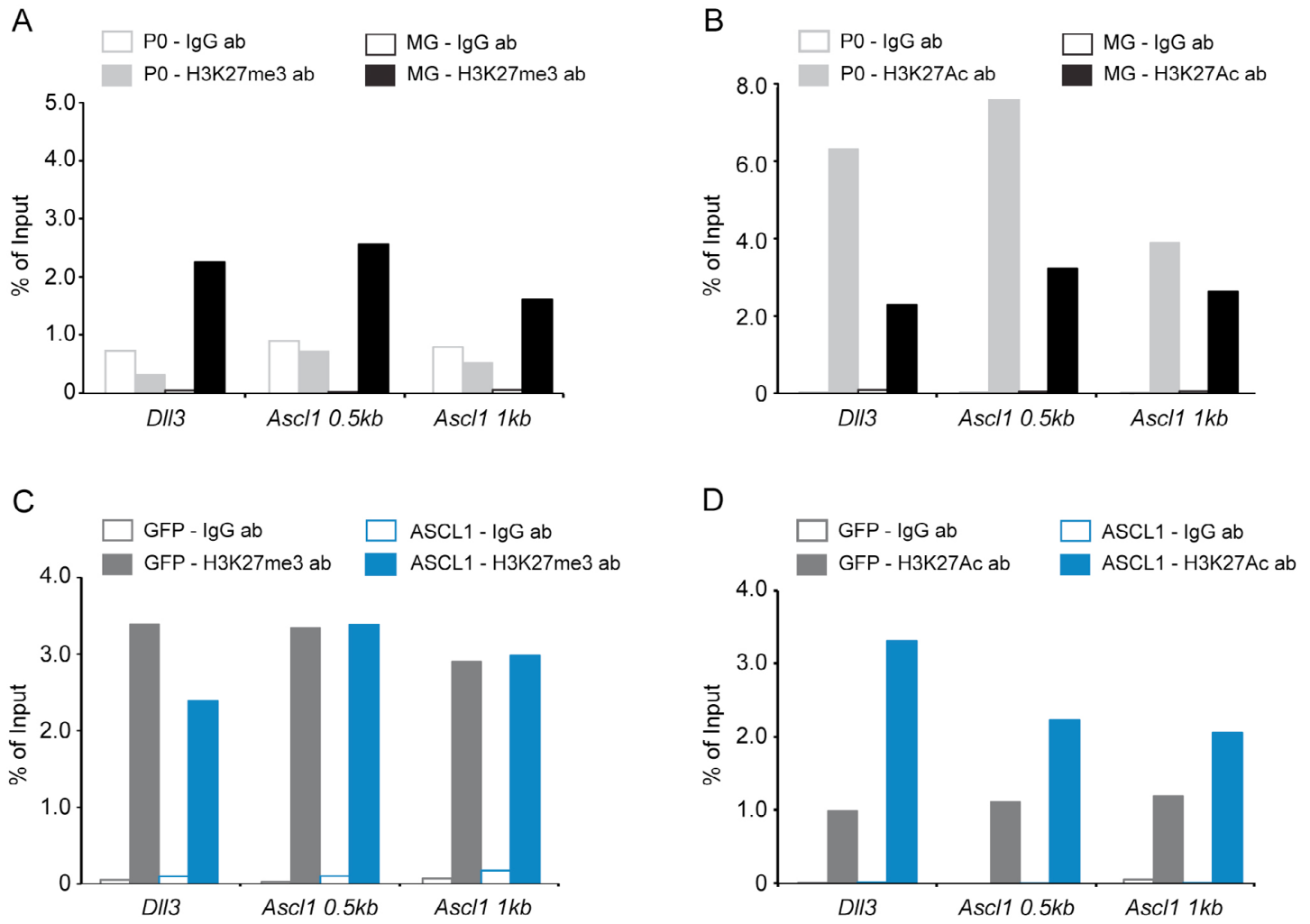

Fig S5. The *Ascl1* promoter is repressed during MG development and partially remodeled by *ASCL1* expression. Related to Fig. 5. ChIP for H3K27me3 or H3K27Ac versus IgG control antibodies at two locations in the *Ascl1* 5′ promoter, 500 bp and 1 kb upstream of the transcription start site. *Dll3* is included as a control progenitor gene locus consistent with Fig. 5. (**A**,**B**) The Ascl1 promoter shows an increase in tri-methylation (A) and a decrease in acetylation (B) between P0 progenitors and P12 MG. (**C**,**D**) ASCL1 infection of MG at 4 dpi reverses the acetylation (D), but not the tri-methylation (C) trend.

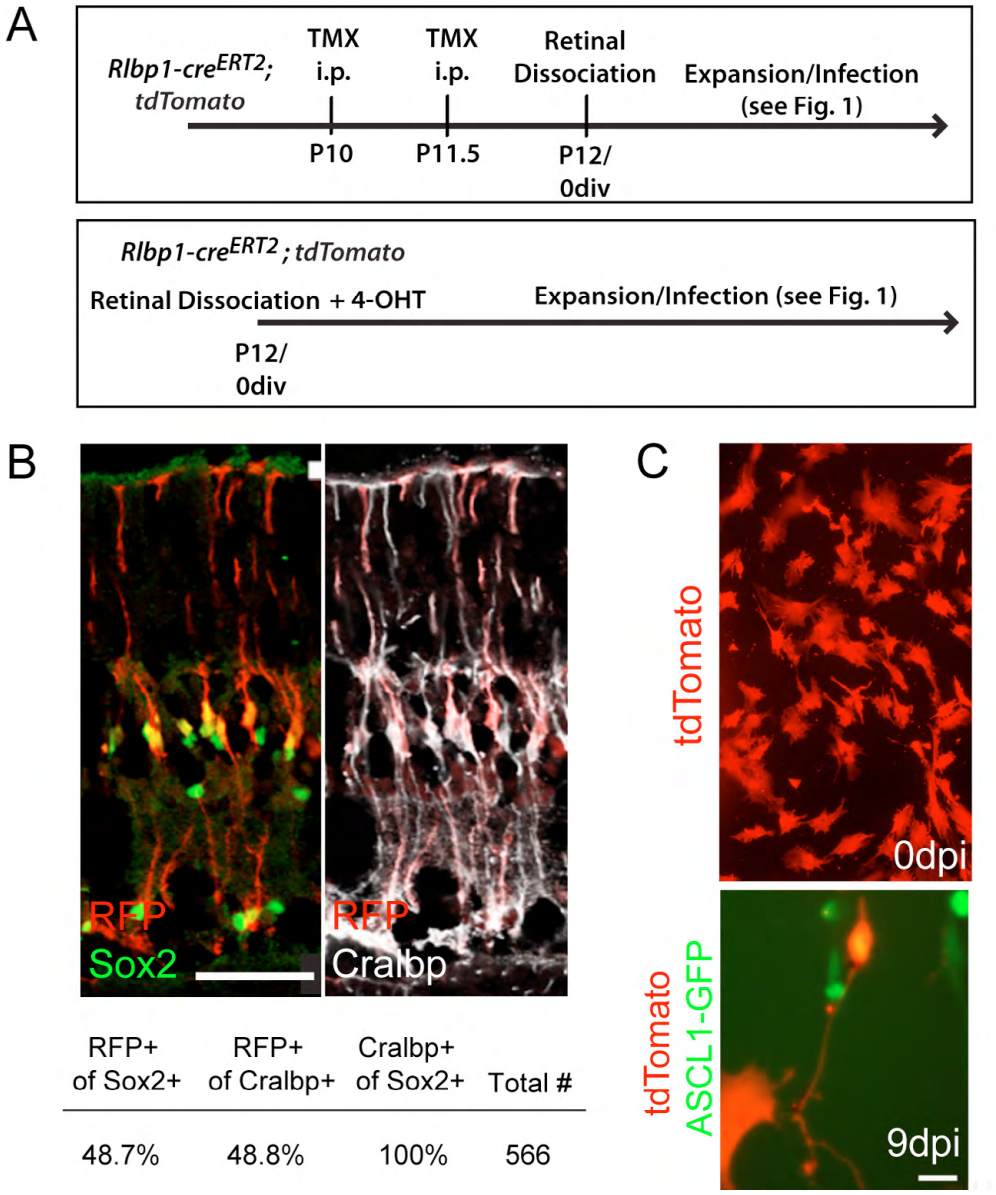

Fig. S6. Genetic fate mapping of cells derived from *Rlbp1-cre^{ERT2};tdTomato* P12 MG. Related to Fig. 7. (**A**) Experimental diagram. *Rlbp1-cre^{ERT2};R26-flox-stop-tdTomato* retinas express tdTomato in Cralbp+ MG after tamoxifen (TMX) administration. Tamoxifen was injected at P10 and P11.5 or 4-hydroxy-tamoxifen (4-OHT) was added to MG cultures to drive cre into the nucleus. MG were grown and infected as described in Fig. 1. (**B**) RFP+ cells in P12 *Rlbp1-cre^{ERT2};tdTomato* retinal cryosections colabel with glial markers Sox2 and Cralbp. Approximately 50% of RFP+ cells label with glial markers when TMX is administered *in vivo* (A, upper panel). (**C**) Dissociated P12 *Rlbp1-cre^{ERT2};tdTomato* ASCL1-infected MG cultures. By 9 dpi, ASCL1-GFP+tdTomato+ cells with a neuronal appearance are observable. Scale bars: 20 μm (C); 50 μm (B).

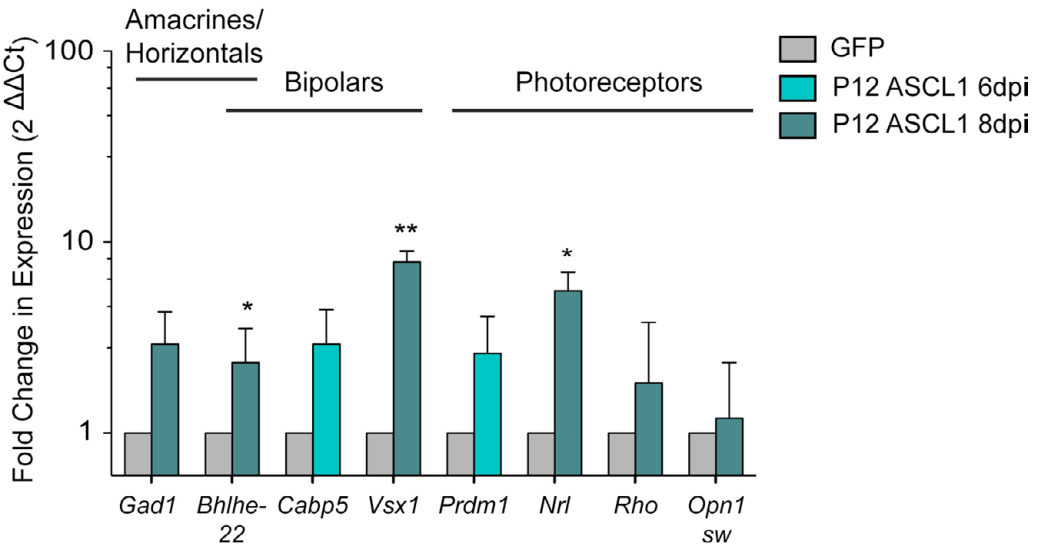

Fig. S7. Expression of late retinal neuronal genes. Related to Fig. 8. Genes specific to differentiated bipolar and amacrine cells are upregulated in P12 ASCL1-infected MG by qPCR. Data are mean ± s.e.m. Student's *t*-test, **P*<0.05, ***P*<0.01.

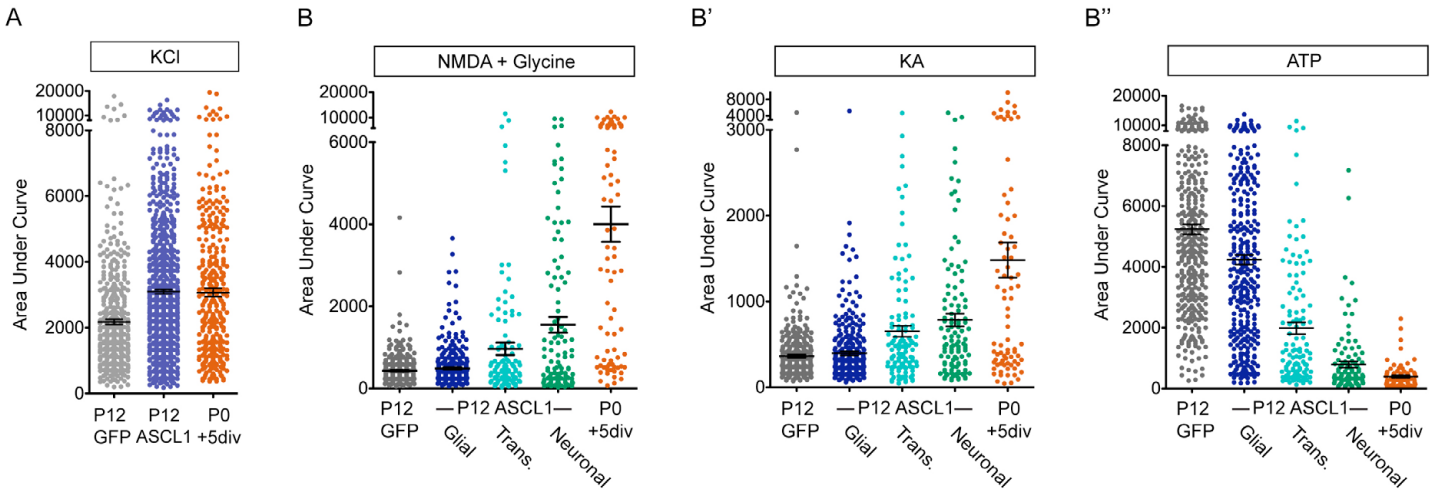

Fig. S8. Morphology of ASCL1-infected MG is associated with calcium responsiveness. Related to Fig. 9. (**A**) ΔF340/380 responses to KCl application, as measured by area under the curve. (**B-B''**) Classification of ASCL1-infected MG from Fig. 9 by morphology (glial, transitional or neuronal). Neuronal- and transitional-like cells were more responsive to NMDA (B) and KA (B') and less responsive to ATP (B'') compared with cells with a glial appearance.

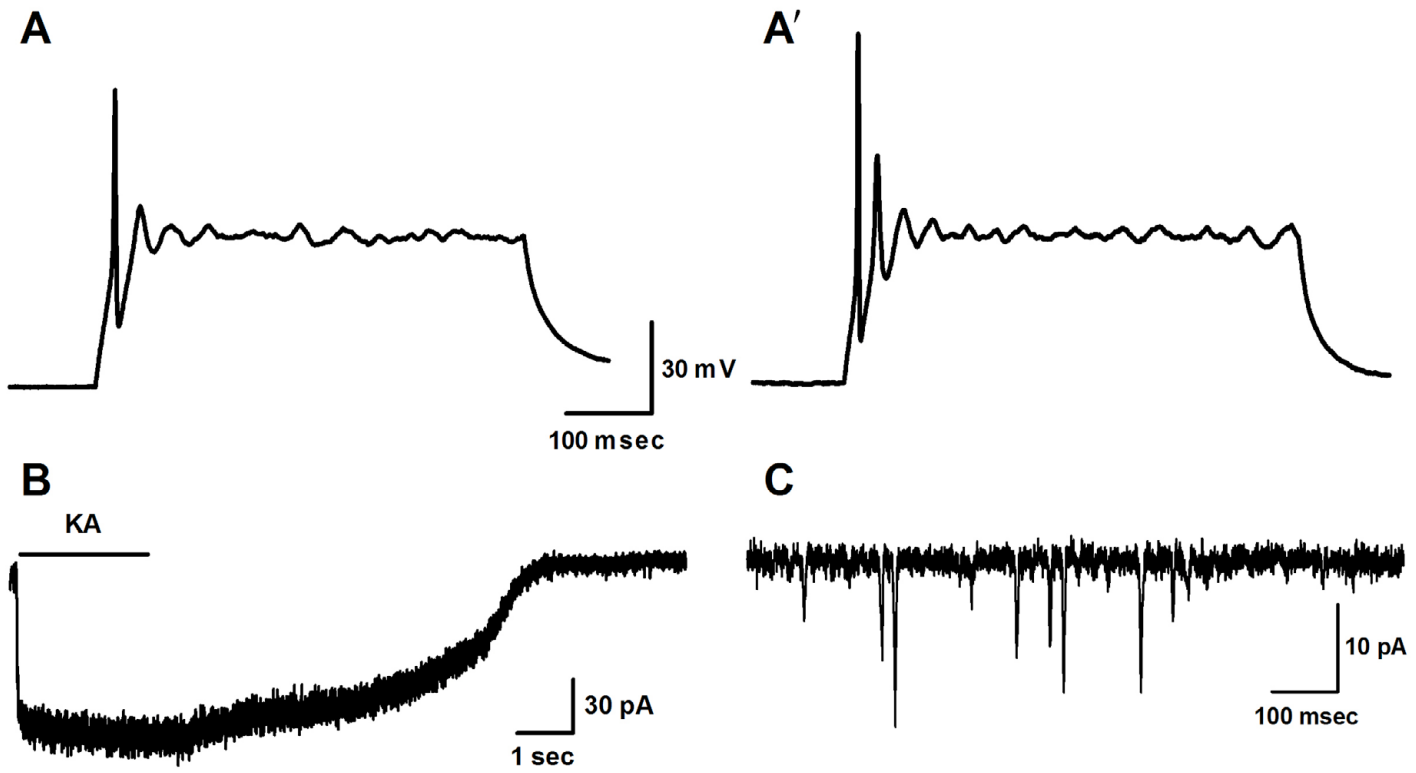

Fig. S9. ASCL1-infected MG-derived cells have neuron-like electrophysiological responses. Whole-cell patch clamp. (**A**,**A′**) Current clamp recordings of action potentials evoked in two different ASCL1– GFP+ cells with neuronal morphology (15 dpi) in response to a 40 pA current step lasting 500 mseconds. (**B**) Voltage clamp recording of response (same cell as in A) to a 3-second application of 50 µm kainate (KA). (**C**) Voltage clamp recording of spontaneous miniature postsynaptic potentials in a third ASCL1– GFP+ cell (20 dpi) co-cultured for 18 days with retinal neurons dissociated from P0 animals.

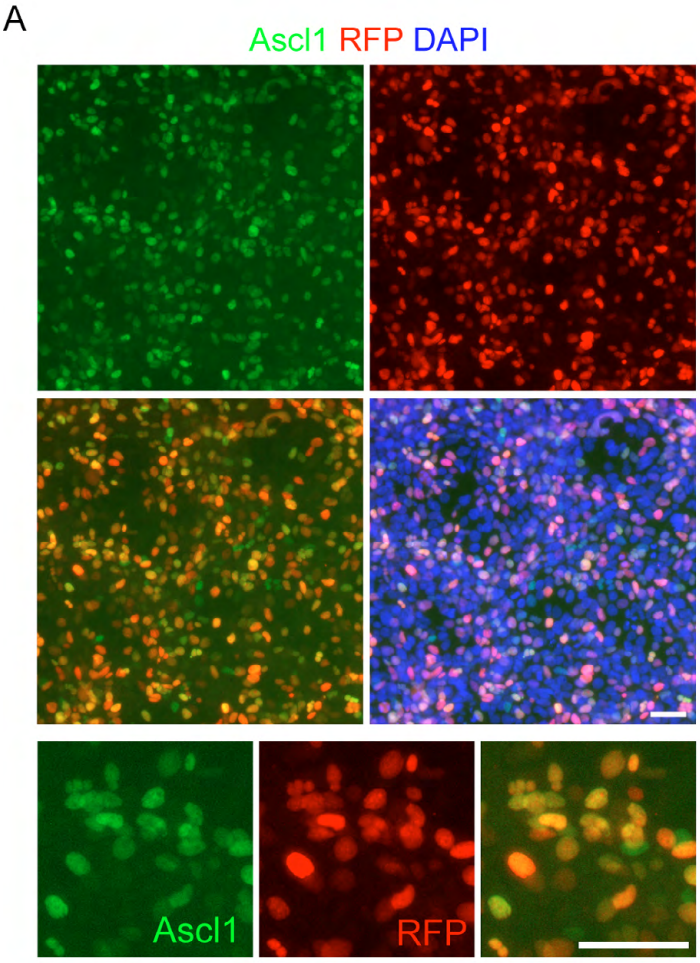

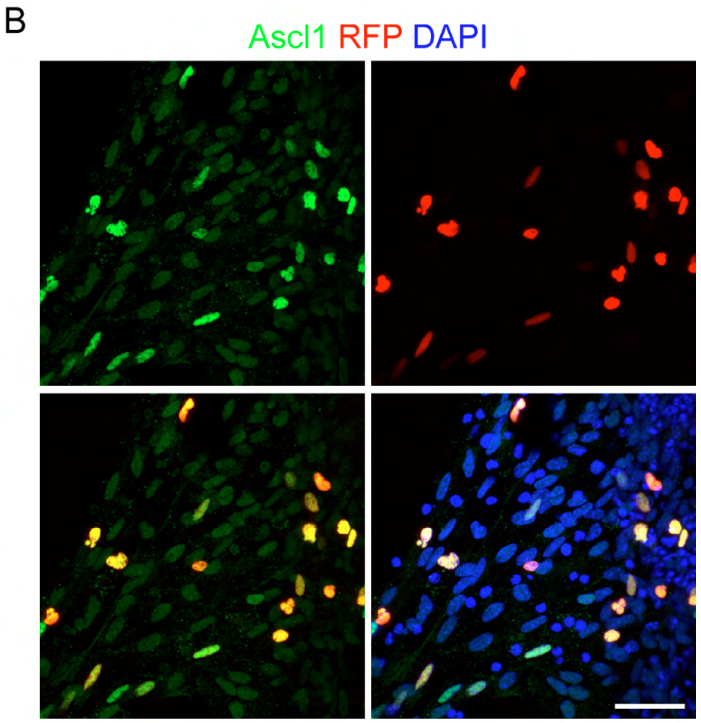

# RFP+ /Ascl1-	# Ascl1+ /RFP-	Total #	% RFP+ of Ascl1+	% Ascl1+ of RFP+
14	26	887	97.0	98.4

Fig. S10. Validation of *tetO-hASCL1-IRES-mCherryn* plasmid expression. Related to Fig. 10. (**A**) Stable rtTA-expressing HEK293T cells were infected with *tetO-hASCL1-IRES-mCherryn* lentiviral particles in the presence of 750 ng/ml doxycycline and fixed at 3 dpi. Ninety-seven percent of ASCL1+ cells immunolabeled for RFP and 98.4% of RFP+ cells labeled with Ascl1, indicating that mCherry/RFP can reliably be used as a marker for ASCL1 expression. (**B**) Ascl1 and mCherry markers colocalize in *αPax6-cre;R26-stop-flox-rtTA* P12 retinal explants infected with *tetO-hASCL1-IRES-mCherryn.* Scale bars: 50 μm (A); 100 μm (B).

Table S1. Primer sequences used for qPCR and ChIP analyses

qPCR primers

Gene name	F sequence (5′ to 3′)	R sequence (5′ to 3′)
Actb	GGCTGTATTCCCCTCCATCG	CCAGTTGGTAACAATGCCATGT
ASCL1 (human)	CATCTCCCCCAACTACTCCA	CAGTTGGTGAAGTCGAGAAGC
Atoh7	ATCACCCCTACCTCCCTTTCC	CGAAGAGCCTCTGCCCATA
Bhlhe22	TGAACGACGCTCTGGATGAG	GGTTGAGGTAGGCGACTAAGC
Cabp5	ATGAGAACGATGGGTTACATGC	CACGGCCACCAAGGTTCATT
Cralbp	GGCACTTTCCGCATGGTTC	CCGGGTCTCCTCCTTTTCAT
Crx	TCTCTCACCTCAGCCCCTTAT	ACCCACTGAAATAGGAACTTGGA
Dll1	CAGGACCTTCTTTCGCGTATG	AAGGGGAATCGGATGGGGTT
Dll4	TTCCAGGCAACCTTCTCCGA	ACTGCCGCTATTCTTGTCCC
Fabp7	GGACACAATGCACATTCAAGAAC	CCGAACCACAGACTTACAGTTT
Fgf15	TCACATGGACCCTGTTGTGT	CAGCAGCCTCCAAAGTCAGT
Foxn4	CATGAAGGAGCACTTCCCCTA	TTTCCGGGCGGTCTGAGAT
Gad1	CACAGGTCACCCTCGATTTTT	ACCATCCAACGATCTCTCTCATC
Gadd45g	GGGAAAGCACTGCACGAACT	AGCACGCAAAAGGTCACATTG
Hes5	AGTCCCAAGGAGAAAAACCGA	GCTGTGTTTCAGGTAGCTGAC
Hes6	ACCACCTGCTAGAATCCATGC	GCACCCGGTTTAGTTCAGC
Heyl	CAGCCCTTCGCAGATGCAA	CCAATCGTCGCAATTCAGAAAG
Hmgb3	AGGTGACCCCAAGAAACCAAA	GCAAAATTGACGGGAACCTCTG
Isl1	TATCCAGGGGATGACAGGAAC	GCTGTTGGGTGTATCTGGGAG
Mfng	ATGCACTGCCGACTTTTTCG	CCTGGGTTCCGTTGGTTCAG
Myb	GAGCACCCAACTGTTCTCG	CACCAGGGGCCTGTTCTTAG
Mycn	ACCATGCCGGGGATGATCT	ATCTCCGTAGCCCAATTCGAG
Neurod1	ATGACCAAATCATACAGCGAGAG	TCTGCCTCGTGTTCCTCGT
Neurod4	AGCTGGTCAACACACAATCCT	GTTCCGAGCATTCCATAAGAGC
Neurog2	AACTCCACGTCCCCATACAG	GAGGCGCATAACGATGCTTC
Nrl	TCCCAGTCCCTTGGCTATGG	CACCGAGCTGTATGGTGTG
Olig2	GCTCACCAGTCGCTTCATCT	GCGCGAAACTACATCCTCAT
Opn1sw	CAGCATCCGCTTCAACTCCAA	GCAGATGAGGGAAAGAGGAATGA
Opn2	CCCTTCTCCAACGTCACAGG	TGAGGAAGTTGATGGGGAAGC
Otx2	TATCTAAAGCAACCGCCTTACG	AAGTCCATACCCGAAGTGGTC
Prdm1	TTCTCTTGGAAAAACGTGTGGG	GGAGCCGGAGCTAGACTTG
Prox1	AGAAGGGTTGACATTGGAGTGA	TGCGTGTTGCACCACAGAATA
Sfrp2	CGTGGGCTCTTCCTCTTCG	ATGTTCTGGTACTCGATGCCG
Slc1a3	ACCAAAAGCAACGGAGAAGAG	GGCATTCCGAAACAGGTAACTC
Tubb3	TAGACCCCAGCGGCAACTAT	GTTCCAGGTTCCAAGTCCACC
Turbo-Gfp	GACCAAGACTGGGGAGATCA	ACAGCCACAATGGTGTCAAA
Vsx1	GAGGCACAGGACGGTTTTCA	AGCTCTGTTTTCGCAGCCA

ChIP primers

Gene name	F sequence (5′ to 3′)	R sequence (5′ to 3′)
MyoD	GGCTTTTAGGCTACCCTGGAT	TGGTGAAGAAAGCAGTCGTG
Hes5	TTCCCACAGCCCGGACATT	GCGCACGCTAAATTGCCTGTGAAT
Dll1	AGCTCTTTCTCTCCGCATTG	CTGTTATTGTGCGAGGCTGA
Hes6	CATGTCAATGCACCGATTGGC	GCCTAAGTGGCAGGAGGTC
Dll3	TGCCCGAAGACTGAAGACTAATT	TGGGCTCAGGAAGGTGTGA
Ascl1 0.5 kb	GCCACTCCTCTGAAAGATGC	TTTATTCCACACAGCCCACA
Ascl1 1 kb	CAGGGAAGGGTTTAGGCAGA	CTCTCCCCTCCTACCTTCCT

Table S2. GO analysis of most highly regulated genes after Ascl1 infection of P12 MGs

GO term	Description	*P*-value	FDRq-value	Enrichment
GO:0007399	nervous system development	1.14E-15	1.29E-11	4.95
GO:0060284	regulation of cell development	1.37E-14	7.71E-11	2.48
GO:0045664	regulation of neuron differentiation	1.81E-14	6.81E-11	2.97
GO:0050767	regulation of neurogenesis	3.41E-14	9.63E-11	2.76
GO:0023051	regulation of signaling	8.08E-14	1.82E-10	2.18
GO:0050804	regulation of synaptic transmission	8.42E-14	1.58E-10	5.32
GO:0051969	regulation of transmission of nerve impulse	9.50E-14	1.53E-10	4.98
GO:0010646	regulation of cell communication	9.96E-14	1.40E-10	2.17
GO:0048731	system development	1.08E-13	1.35E-10	3.29
GO:0050793	regulation of developmental process	2.17E-13	2.45E-10	2.04
GO:0051960	regulation of nervous system development	2.89E-13	2.97E-10	2.59
GO:0071840	cellular component organization or biogenesis	3.90E-13	3.67E-10	1.4
GO:0048869	cellular developmental process	1.03E-12	8.97E-10	2.49
GO:0007275	multicellular organismal development	1.26E-12	1.01E-09	2.98
GO:0031644	regulation of neurological system process	1.45E-12	1.09E-09	4.56
GO:0051239	regulation of multicellular organismal process	1.63E-12	1.15E-09	2.03
GO:0032502	developmental process	2.91E-12	1.93E-09	2.02
GO:0016043	cellular component organization	3.94E-12	2.47E-09	1.39
GO:0044708	single-organism behavior	4.43E-12	2.63E-09	3.89
GO:0045595	regulation of cell differentiation	5.65E-12	3.19E-09	2.19
GO:0042391	regulation of membrane potential	5.89E-11	3.17E-08	3.01
GO:0007610	behavior	8.25E-11	4.23E-08	3.42
GO:0022402	cell cycle process	1.94E-10	9.51E-08	1.85
GO:0048856	anatomical structure development	2.82E-10	1.33E-07	1.92
GO:2000026	regulation of multicellular organismal development	4.78E-10	2.16E-07	2
GO:0044057	regulation of system process	5.54E-10	2.41E-07	3.11
GO:0007219	Notch signaling pathway	7.24E-10	3.03E-07	14.14
GO:0048522	positive regulation of cellular process	8.41E-10	3.39E-07	1.57
GO:0030154	cell differentiation	1.34E-09	5.23E-07	2.41
GO:0007268	synaptic transmission	1.36E-09	5.11E-07	4.08
GO:0050806	positive regulation of synaptic transmission	5.72E-09	2.08E-06	8.07
GO:0031646	positive regulation of neurological system process	5.85E-09	2.06E-06	7.44
GO:0048646	anatomical structure formation involved in morphogenesis	6.14E-09	2.10E-06	3.27
GO:0051128	regulation of cellular component organization	6.88E-09	2.28E-06	1.54
GO:0044767	single-organism developmental process	1.17E-08	3.76E-06	1.96
GO:0007049	cell cycle	1.34E-08	4.20E-06	1.8
GO:0051971	positive regulation of transmission of nerve impulse	1.36E-08	4.14E-06	7.63
GO:0048518	positive regulation of biological process	1.67E-08	4.97E-06	1.61
GO:0006260	DNA replication	1.72E-08	4.99E-06	2.7